1966

Diffusional drop growth in a supersaturated atmosphere

John C. Carstens
Missouri University of Science and Technology, carstens@mst.edu

Department: Physics

DIFFUSIONAL DROP GROWTH IN A SUPERSATURATED ATMOSPHERE

BY

JOHN CARSTENS

A

DISSERTATION

submitted to the faculty of the

UNIVERSITY OF MISSOURI AT ROLLA

in partial fulfillment of the requirements for the

Degree of

DOCTOR OF PHILOSOPHY

Rolla, Missouri

1966

Approved by

J. W. Rivers (advisor) Harris B. Lund

James L. Kassner, Jr. Joseph E. Willett

Charles A. Johnson Hughes M. Zerr

Richard Anderson

ABSTRACT

The effect which a growing droplet has on the supersaturated atmosphere surrounding it is analyzed by assuming a macroscopic diffusional growth mechanism involving both heat and vapor. The problem is solved, for cloud-chamber conditions, first for very short times assuming a fixed radius, and then for longer times assuming the establishment of "quasi" steady-state conditions. Knowledge of the way in which droplet growth affects supersaturation is important in the evaluation of nucleation rates.

ACKNOWLEDGMENTS

The author wishes to thank Dr. J. L. Rivers for his advice and encouragement in the completion of this problem. Thanks are also due to Dr. J. Kassner who suggested the problem, and continued to show a helpful interest in it, and to his staff of graduate students who allowed the author free use of their time and equipment.

This research was supported by the Atmospheric Sciences Section of the National Science Foundation, NSF Grant GP - 2893.

TABLE OF CONTENTS

LIST OF ILLUSTRATIONS

LIST OF TABLES

CHAPTER I

Introduction:

For the past several years a primarily experimental endeavor has been underway with the atmospheric physics group at the University of Missouri at Rolla to measure homogeneous nucleation rates using a specialized cloud-chamber.[1] The overall purpose has been to provide various theories with a meaningfully accurate value of this rate with which different theoretical expressions could be compared. Direct comparison, however, is thwarted by the fact that while experimentally measured nucleation rates necessarily take place in an atmosphere partially relieved of vapor by droplets themselves, no such depletion is accounted for in the usual theoretical development. Nor is account taken of the evolution of heat from these droplets, which arises from the latent heat deposited by the incoming vapor.

These effects suggest a pragmatic concept: dead space, the space around a droplet where warming and vapor depletion have reduced the supersaturation. We can conceive of such a volume, say V_d, as a spherical region concentric with the droplet, of outer radius d, i.e.

$$V_d = \frac{4}{3}\pi d^3.$$

Inside this region a supersaturation of unity is imagined to exist, so that the nucleation rate is zero. Outside the

region ($r > d$) the bulk supersaturation, $S(R,t)$, is imagined to exist. The validity of an experimental-theoretical comparison presupposes an estimate of the dead space magnitude as well as an assessment of its effect on the nucleation rate. Analyses of this sort have been made by Grayson[2] in this laboratory, and elsewhere both experimentally and theoretically.[3] The present paper addresses itself to a theoretical estimation of the dead space.

Distribution of Drops in a Cloud-Chamber: Competition Effects:

We begin by considering specifically the situation existing in the sensitive volume of a cloud-chamber during a controlled expansion. We will further specify the atmosphere to be composed of a vapor in dilute solution with a noncondensible gas. It is well-known that such an atmosphere will, upon expansion, tend to divest itself of excess vapor by forming droplets either on "nucleation centers", such as ions or dust particles, or simply spontaneously, i.e. in the homogeneous nucleation here under consideration. We are led, then, to consider generally the emergence of $I(S)$ nucleation centers (representing "potential" droplets) per unit volume per unit time attributable to the continuing controlled expansion of the chamber above a certain critical supersaturation S_c. Here I = nucleation rate in droplets/cm^3/sec, S = supersaturation, and t = time. A typical droplet of radius $a(t)$ is surrounded by a random

collection of other droplets, nucleating and growing.

If we have a large number of drops, either by virtue of a large sensitive volume, or by an average over a large number of identical expansions, every sufficiently large volume element will look like every other element. We can then speak of a number dn(m) per unit volume of droplet masses between m and m + dm, where m is the mass of the drop. Furthermore, if the history of the drop is known, this number can be specified at a time t. dn should be inversely proportional to the rate, R(m,t), of droplet growth at time t, and directly proportional to the number produced time t' ago which have attained the specified size range. We have:

$$\frac{dn(m)}{dm} = \frac{k\, I(s,t')}{R(m,t)}$$

where since,

$$\frac{dm}{dm}\, R(m,t) = \frac{dm}{dm}\,\frac{dm}{dt} = k\, I(s,t')$$

$$\frac{dm}{dt} = k\, I(s,t')$$

then, k = 1.

So the distribution for drop sizes is given by:

(1.1)
$$\frac{dn(m)}{dm} = \frac{I(s,t')}{R(m,t)}$$

with m and t' connected by:

$$m(t,t') = \int_{t'}^{t} R(m,\tau)\, d\tau$$

If, within the unit volume, S is a function of $\vec{r}$, that is $S = S(\vec{r},t)$, then the above formula is invalid, and I must be replaced by:

$$\int_{\text{unit vol.}} I[S(\vec{r}),t']\,d^3\vec{r}$$

while the rate, R, becomes a function both of the droplet's location and its history. If we now permit ourselves to regard R as independent of $\vec{r}$, the previous population distribution holds, with I replaced by the above integral. This important assumption amounts to the exclusion of "competition effects," i.e. two or more droplets competing for the same vapor, and considerably simplifies the problem of estimating a dead space.

The Diffusion Equations for Drop Growth:

We proceed, then, under the above restrictions, to fix attention on one droplet of this array and examine the effects this droplet may have on its circumambiant atmosphere. We can assure the independence of one droplet from another by describing a sphere around each droplet, the diameter, 2R, of which is roughly equal to the average distance between droplets. Regarding this sphere to be impenetrable (to both heat and vapor), in addition to providing an outer boundary condition for the problem, has the physical significance that only a limited amount of vapor is allotted to the droplet, the rest being appropriated by other droplets in contiguous spheres. When the annular

region at the edge of a given sphere is sensibly affected by events occurring at the droplet, competition is evidently imminent, and the impermeability boundary condition must be abandoned. It may be added that any solution obtained in the noncompetitive regime should be practically indistinguishable from that obtained by letting R go to infinity; nevertheless, the existence of a finite R at least serves to forecast graphically the onset of competition, and may as well provide a "point of departure" for the treatment of competition.

Turning to that region of the R-sphere which is affected by the presence and growth of the droplet, we expect to observe the double diffusion of vapor toward the drop, and heat, given off by the condensing vapor, away from it. In brief, the drop acts as a source of heat and a sink of vapor. The amount of vapor available for condensation is a function of the supersaturation, the knowledge of which is, of course, a consequence of solving the vapor-heat diffusion problem. But at the outer edge of the sphere supersaturation is a function of the applied expansion, i.e. of time alone. The same applies to the temperature, T, and the density, ρ. We thus envisage a homogeneously changing $T_o(t)$ and $\rho_o(t)$ upon which is superimposed a nonhomogenous (but spherically symmetric) $T(r,t)$ and $\rho(r,t)$, so that the actual values of these variables may be written:

$$T_o(t) + T(r,t)$$

$$\rho_o(t) + \rho(r,t).$$

Now the chamber achieves supersaturation by an expansion which occurs quickly enough so that central portions of the chamber remain "insulated" from the influx of heat from the outer walls, i.e. unit volumes in the sensitive volume stay adiabatic.[4] Then, since no heat flows in or out of a unit volume in this region, we can imagine the cooling to be effected by a homogeneous "sink" term. The sudden drop in vapor density can likewise be ascribed to a sink term, so that the two governing diffusion equations can be written:

$$\nabla\left[D(T)\,\nabla\rho\right] = \frac{\partial\rho}{\partial t} - F_\rho(t)$$

$$\nabla\left[K(T)\nabla T\right] = \frac{\partial T}{\partial t} - F_T(t)$$

where, D(T) = diffusion coefficient,

k(T) = diffusivity,

and, F_ρ and F_T are sink terms.

At the surface of the drop the net influx of molecules must be the difference between those condensing and those evaporating. If an overall temperature T(a,t) can be associated with the drop (any diffusion inside the drop occurring instantaneously), this evaporation is expressible in terms of the condensation to the droplet under equilibrium conditions. Likewise at the droplet surface we must have a power balance equating incoming heat, due to condensation, with the outgoing diffusing heat plus the heat used in raising the temperature of the drop. The latter condition

can be written:

$$\tfrac{1}{3}\rho_w\, a(t)\, c_w \frac{dT(a,t)}{dt} = l\, D \nabla \rho \Big|_{r=a} + K \nabla T \Big|_{r=a}$$

where, ρ_w = density of liquid in drop,

a(t) = radius of drop at time t,

l(T) = latent heat of condensation of vapor,

K(T) = thermal conductivity of medium in which droplet is immersed,

and, c_W = specific heat of liquid.

Following Mason[5] the former condition will be replaced by requiring ordinary equilibrium between temperature and vapor density to prevail at the droplet's surface. This relationship is postulated to be of the form:

$$\rho = \sum_{m=0}^{\infty} a_m T^m$$

The equation for a(t) is:

$$\rho_w \frac{da(t)}{dt} = D \nabla \rho \Big|_{r=a}$$

Finally the initial condition must be specified in terms of the history of the droplet. The above equations, being macroscopic, purport only to describe the physical situation existing when a(t) exceeds the mean free path, λ, associated with the surrounding gas molecules. The implication is that this description "takes over" as soon as $a(t) \sim \lambda$. At this point of time we will provisionally

assume a reasonable initial condition has been presented to us, representing the tail-end of the solution of the problem worked out by kinetic theory methods, or by some other means valid in that region. Collecting equations:

(1.2) $$\nabla[D(T)\nabla\rho] = \frac{\partial\rho}{\partial t} - F_\rho(t)$$

(1.3) $$\nabla[k(T)\nabla T] = \frac{\partial T}{\partial t} - F_T(t)$$

(1.4) $$T(0,r) = f_T(r)$$

(1.5) $$\rho(0,r) = f_\rho(r)$$

(1.6) $$\nabla\rho\,|_{r=R} = \nabla T\,|_{r=R} = 0$$

(1.7) $$\rho[a(t),t] = \sum_m a_m T^m\,|_{r=a(t)}$$

(1.8) $$\frac{dT}{dt}\Big|_{r=a(t)} = (\alpha\nabla\rho + \beta\nabla T)\,|_{r=a(t)}$$

(1.9) $$\rho_w \frac{da}{dt} = D(T)\,\nabla\rho(r,t)\,|_{r=a(t)}$$

where,

$$\alpha = \frac{D\ell}{c_w\rho_w a(t)} \qquad \beta = \frac{K}{c_w\rho_w a(t)}$$

and D, K, k, and ℓ are all functions of T.

Aside from the assumptions already introduced, it is important to note that this description neglects (1) convective effects, (2) the effect that heat diffusion has on mass diffusion, and (3) the effect that mass diffusion has on heat diffusion. The last two assumptions, due to Neiburger and Chien[6], are a consequence of the assumed diluteness of the vapor.

Evaluation of the Dead-space Parameter:

Given a solution to the above equations, we will be in a position to evaluate the dead-space parameter V_d. This is easily done if $T(r,t)$ and $\rho(r,t)$ are known, since these determine the supersaturation. If we suppose $S(r,t)$ to be obtained from T and ρ, we can evaluate V_d according to:

$$I[S(t),R]\left[\tfrac{4}{3}\pi R^3 - V_d(t)\right] = \int_{a(t)}^{R} I[S(t,r)]\, 4\pi r^2 dr$$

$$\therefore V_d = \tfrac{4}{3}\pi R^3 - \frac{4\pi}{I[S(t,R)]}\int_{a(t)}^{R} I(S,r) r^2 dr \qquad (1.10)$$

Thus a knowledge of V_d follows directly from a solution of the diffusion equations. To solve this rather complicated set of equations some assumptions must be invoked. The next chapter gives a brief account of some customary simplifying assumptions which allow a solution to the general diffusion problem.

CHAPTER II

The object of this chapter is to present a general, if somewhat brief, survey of popular simplifying assumptions used in the solution of diffusional droplet growth problems, along with some of their implied solutions. In pursuing this object we will be led to a closer examination of the origin of the initial condition posited in the first chapter. Details of droplet growth, insofar as they are describable by a macroscopic diffusional mechanism, are hereafter assumed to be adequately represented by the equations collected in Chapter I.

Probably the most widely used assumption (the so-called "quasi steady-state" assumption) secures considerable simplification by setting time derivatives of the dependent variables equal to zero:

$$\frac{\partial \rho}{\partial t} = \frac{\partial T}{\partial t} = 0.$$

Its justification, according to Riess and La Mer, appeals to the fact that when material diffuses from an infinite region to a single sink..."the flux of diffusing material through any surface in the diffusion field is much greater than the rate of change of concentration on that surface."[7] A more extensive discussion of this point is given by Kirkaldy who especially investigates the spherically symmetric case.[8]

Of the many quasi steady-state calculations

performed,[9,10,11,12,13] Mason's seems to be typical, and the following treatment is based on his assumptions. Mason "starts" the droplet at its critical radius, that is the radius at which it is in unstable equilibrium with its atmosphere. He introduces values of the diffusion constants, k and D, corrected for the region $a \sim \lambda$, as constants appropriate to the average radius in a step-wise calculation. The macroscopic equations used by Mason are, in the notation of the present work,

$$\frac{dF_T}{dt} = \frac{dF_\rho}{dt} = \nabla^2 T = \nabla^2 \rho = 0$$

$$D\ell \nabla\rho\big|_{r=a} = K \nabla T\big|_{r=a} \neq 0$$

$$\rho(a) = \rho_R \exp\left(\frac{\ell}{R}\,\frac{T-T_R}{T T_R}\right)\Bigg|_{r=a} = \sum_m a_m T^m(a).$$

The last equation is obtained by regarding the vapor as an ideal gas, and integrating the Clausius-Claperyon equation between ρ_R, $\rho(r)$ and T_R, T, where $\rho(a)$ is the vapor density at the droplet, and ρ_R that at the outer sphere. The steady-state solutions are:

$$\rho(r) = \rho_R - \frac{a}{r}\,\frac{R-r}{R-a}\left[\rho_R - \rho(a)\right]$$

$$T(r) = T_R - \frac{a}{r}\,\frac{R-r}{R-a}\left[T_R - T(a)\right]$$

(The above are valid for Mason's case, $R=\infty$, since $\lim_{R\to\infty}$ $(R-r)/(R-a) = 1$)

Buecher has indicated that, in temperature ranges ordinarily of interest, terms to T^2 in the vapor equilibrium condition yield excellent accuracy.[14] Hence we can put:

$$\rho(a) = \sum_{m=0}^{\infty} a_m T^m(a) \cong \left(\ell T^2 + bT + c \right)_{r=a}$$

Substitution of $\rho(r)$ and T(r) into the power balance equation, $-D\ell \nabla\rho|_{r=a} = K \nabla T|_{r=a}$ gives:

$$\frac{\rho_R - \rho(a)}{T_R - T(a)} = -\frac{K}{D\ell}.$$

Treating (R-a)/R as constant, since its variation is of the order of $\Delta a/R^2$ which is usually small (this becomes exact for $R = \infty$), we obtain from,

$$\rho(a) = \ell T^2(a) + bT(a) + c$$

an expression for the change in radius squared:

$$\frac{da^2}{dt} = \frac{\alpha_D - b\alpha_K}{2} + \frac{1}{2}\left[(\alpha_D - b\alpha_K)^2 - 8\ell^2 \alpha_K^3 T_R \right]^{\frac{1}{2}}$$

where, $\alpha_D = \frac{R-a}{RD}$ and, $\alpha_K = \frac{R-a}{RK}$

(Here again some average value of the radius, a, must be taken, or else set a = 0 which is valid for $R = \infty$). An areal dependence of the form,

$$\text{drop area} = 4\pi a_0^2 + t \cdot \text{const.}$$

is obtained in agreement with others.[15,16,17]

Mason proceeds to estimate overall supersaturation change by applying quasi steady-state theory during short time intervals. After each interval he computes the vapor extracted from the system as well as the heat imparted to it. From this he calculates a new, homogeneous supersaturation. His neglect of a radial dependence of S, discussed in Chapter I of this work, is regarded as an approximation. Mason compared reductions in nucleation rate with Frey's experiments[18] in which a supersaturation of 10.4 produces a maximum drop concentration of 1.8×10^6 drops/cm^3, as compared with Mason's 3.8×10^6 drops/cm^3.

Other authors, employing quasi steady-state techniques in the macroscopic regime, attempt a more explicit connection with initial stages of growth occurring in the microscopic regime[19,20,21]. Bagge, Becker, and Bekow[22], for example, resort to kinetic theory methods to calculate the net molecular flux associated with a drop of macroscopic size. To do this they describe a sphere of radius $a + \lambda$ concentric to the droplet, where λ is the mean free path. Assuming the absence of collisions inside this sphere, they calculate the difference between the molecular flux emanating from the inside of the spherical surface toward the droplet, and the evaporational flux originating at the surface of the droplet. The incoming flux is evaluated as if the vapor concentration were homogeneous, and the vapor an ideal gas, beyond $a + \lambda$. The departing flux is evaluated by assuming it to be the equilibrium flux at the

drop temperature. Identical flux calculations are explained more fully in Buecher's thesis[23]. The difference in these fluxes, S, is used in:

$$S = -4\pi D\left[(a+\lambda)^2 \frac{d\rho}{dr}\Big|_{r=a+\lambda}\right]$$

to evaluate the term in brackets. This term is then shown to match the usual gradients when $r >> \lambda$, so that the "microscopic" regime is connected continuously to the "macroscopic".

A more detailed analysis has been attempted by Monchick and Riess[24] who did not assume a homogeneous vapor concentration beyond $r + \lambda$, but instead used a non-equilibrium concentration. This led to a departure from the usual radial growth law of the form:

$$\frac{da}{dt} \propto \frac{m\nu}{1 + \frac{a^2}{a+\lambda}\frac{\nu}{D}}$$

where, $\nu = \frac{1}{4} m \bar{v}$ = collision frequency in molecules/area,

and m = concentration of molecules,

$\bar{v}$ = average molecular speed.

If D is taken to be $(n\bar{v}\lambda)/3$, the growth law expressing constant areal velocity is confirmed for $a >> \lambda$.

Another method attempts to incorporate the moving boundary condition directly into the diffusion equation by the introduction of an independent variable: $\xi = r^m / t^n$. If the variable ξ is evaluated at a moving boundary, e.g. $r = a(t)$, an attempt can be made to choose n or m so that ξ is constant, and the transformed problem is reduced to one

with a fixed boundary. The new variable transforms the diffusion operator,

$$\alpha \nabla^2 - \frac{\partial}{\partial t}$$

to,

$$\frac{m^2 r^m}{t^m} \frac{\partial^2}{\partial \xi^2} + m(m+1) \frac{\partial}{\partial \xi} + \frac{m r^2}{\alpha t} \frac{\partial}{\partial \xi} .$$

This expression can be put solely in terms of ξ by letting $2n = m$. Setting $m = 1$ one obtains:

$$\frac{\partial^2}{\partial \xi^2} + \left(\frac{2}{\xi} + \frac{\xi}{2\alpha} \right) \frac{\partial}{\partial \xi} .$$

It is interesting to note that the relation $2n = m$ requires that we set $\frac{dT(a)}{dt} = 0$, at least if the dependence on ξ alone is to be preserved. Hence insisting that ξ characterize the diffusion problem automatically leads to the boundary conditions:

$$\nabla \rho \big|_{r=a} = \frac{K}{D\ell} \nabla T \big|_{r=a}$$

$$\frac{dF_T}{dt} = \frac{dF_\rho}{dt} = 0$$

$$\frac{d}{dr} \rho(0,r) = \frac{d}{dr} T(0,r) = 0.$$

The transformed equation has the property that a fixed boundary in ξ space implies a moving boundary, proportional to $t^{-1/2}$, in ordinary space. Solutions of the transformed

equation are worked out by Chambre[25], Crank[26], Kirkaldy[27], and Frank[28]. Kirkaldy obtains a result of the form derived from the previously discussed quasi steady-state theory, i.e.

$$\text{drop area} = t \cdot const + 4\pi a_o^2,$$

but he asserts that "this agreement should not be used as a justification for the quasi steady-state theory. The latter remains essentially incorrect mathematically, and gives the correct result only through a lucky combination of compounded errors and suitable geometry."[29]

Another solution, making use of $\nabla^2\rho = 0$, is that of Riess and La Mer[30] who attempt to introduce the moving boundary condition into a solution of $\nabla^2\rho = 0$ for a finite spherical geometry, that is for a drop growing in an impermeable sphere as described in Chapter I. They account for the continuing supersaturation, but neglect the heat flow problem altogether. Their results, applied to aerosols as nuclei indicate that for all but the sparsest concentrations (8 to 10 nuclei/cm^3) spontaneous nucleation is effectively quenched. Their fastest supersaturations build up at a rate of 530 deg/sec which evidently permits extensive diffusion to occur.

Finally mention must be made of Buecher's work in which a solution of the growth problem was performed for droplets of microscopic size.[31] Using simple kinetics, and assuming a homogeneous ideal gas around the drop, Buecher predicted a rapid establishment of a linear growth rate -

the linearity occurring about at the time when temperature stabilization takes place. An attempt will later be made to use Buecher's calculation as an initial condition for the macroscopic problem.

CHAPTER III

In this chapter a solution will be presented which is derived from assumptions based on a re-examination of the physical situation pertaining to cloud-chamber measurements of nucleation rates. The solution will complement those discussed previously, and hopefully set some limits on their validity.

Simplifying Assumptions:

In the first chapter we imagined an array of temporarily independent drops growing and originating in a supersaturated atmosphere. The cloud-chamber is able to produce such an atmosphere quickly, and maintain supercriticality ($S > S_c$) from about .001 to several seconds. Because measurement of nucleation rates becomes questionable for long growth periods, it is the brevity of these supersaturation pulses that claims our attention.

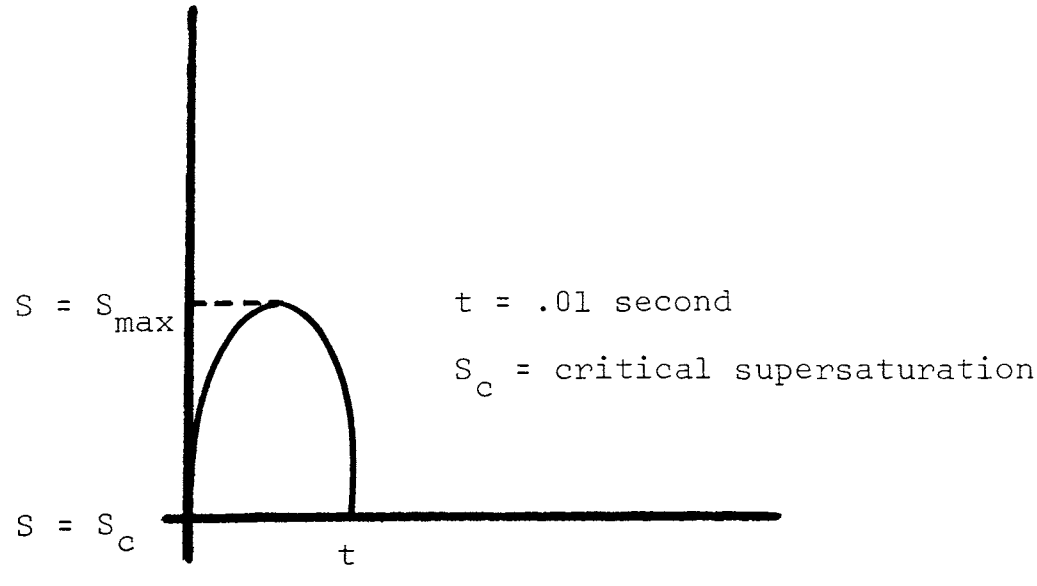

Figure 1. Typical Short Pulse Achieved by Rapid Expansion

Consideration of short pulses such as the one shown above will confine our interest to initial stages of droplet growth and prescribe, to an extent, our choice of simplifying assumptions. The earliest stage of droplet growth extends up to critical size. Farley[32] has estimated its duration to be of the order of 10^{-5} seconds, so that in a typical short pulse critical size is attained almost instantaneously. Subsequent growth, up to macroscopic size, i.e. $a \sim \lambda$, has been treated by Buecher whose results indicate the time to be less than 10^{-4} seconds for a typical expansion.[33] It is clear, then, that sometime near the beginning of the pulse, the supersaturated atmosphere is "presented" with a growing droplet in the vicinity of macroscopic size to which the diffusion equations presumably apply.

As in Chapter II, a simplification is sought which renders the problem solvable while preserving a semblance of physical reality. The discussion of that chapter disclosed a general tendency, in the literature, to assume that transient parts of the total diffusional growth process are comparatively short-lived, and that satisfactory results could be achieved by neglecting this phase of growth altogether. This neglect led to the development of a quasi steady-state theory which incorporated the effect of a moving radius. However it is not apparent that quite short growth periods justify steady-state assumptions. The other

available alternative is to include the partial derivative, $\frac{\partial \rho}{\partial t}$, and the moving radius by the transformation to $\mathfrak{Z}$ space. But it was seen in Chapter II that this forces simplified boundary conditions on the problem, and does not allow the continuing supersaturation to be taken into account.

The above considerations suggest that perhaps a more exact approach to the problem, emphasizing its initial growth stages, is needed. Such a solution, it is hoped, would not only be usable in the analysis of unusually brief pulses, but also capable of evaluating the transient part of prolonged growth.

Unfortunately, as far as this writer can see, retention of all transient terms prevents closed form treatment of a moving radius. Nevertheless the fixed radius assumption frees the rest of the problem from the necessity of further serious simplification, and even this assumption can be amended by noting that the solution so obtained includes a reasonably arbitrary initial condition. Thus the fixed boundary solution, valid for extremely short times during which radial growth is negligible, may lend itself to a step-wise extension to longer times wherein the final solution for any given step constitutes the initial condition for the next. This solution should provide a criterion to determine the advent of steady-state (in which case simpler solutions can be used). We proceed, then, to a solution of the problem with a fixed radius.

Laplace Transform theory provides a straight-forward way of handling both diffusion equations along with their boundary conditions if the problem is linear. This requires that we regard the coefficients D, l, K, and k as average values over ranges of T appropriate to the problem. Also the quadratic,

$$\rho(a) = e T^2(a) + b T(a) + c$$

must be linearized and fitted to the actual vapor equilibrium curve. The steady-state temperature is sufficiently close to the initial drop temperature that the above expression, with e = 0, is a fair approximation.

Initial Conditions:

In keeping with the discussion above, the initial condition will not be introduced in explicit form. The simplest initial condition would be:

$$\rho(0,r) = \rho_R \quad , \quad a \leqq r \leqq R \; ;$$

$$T(0,r) = T_R \quad , \quad a < r \leqq R \; ;$$

$$T(0,r) = T_a \quad , \quad r \leqq a \; ;$$

where T_R and ρ_R are the initial temperature and density respectively, and T_a is introduced to account for droplet heating that may have occurred during its growth history up to macroscopic size. This, of course, neglects heat produced and vapor depleted in the region around the drop.

Boundary Conditions:

As previously mentioned, the outer boundary is an impermeable sphere,

$$\nabla\rho\Big|_{r=R} = \nabla T\Big|_{r=R} = 0.$$

Here T also "builds up" inside the sphere R in the sense that heat exuded by neighboring drops tends to flatten the gradient at R. In effect there is competition among drops not only for vapor, but as well for a cooler "reservoir" to absorb heat produced at the surface r = a. Were it not for the presence of other droplets, such a reservoir would exist at large values of r.

Transformed Problem:

The Laplace transform of a function will be denoted in one of the following ways:

$$\mathcal{L}\,H(t) = h(p) = \bar{H}(p) = \int_0^\infty H(t)\,e^{-pt}\,dt$$

where p is the transform variable, p = x + iy. In spherical coordinates ∇^2 is given by:

$$\frac{\partial^2}{\partial r^2} + \frac{2}{r}\frac{\partial}{\partial r}$$

for radial symmetry. The transformed problem is:

$$D\nabla^2\bar{\rho}(p,r) = p\bar{\rho}(p,r) - \rho(0,r) - f_\rho(p) \tag{3.1}$$

$$k\nabla^2\bar{T}(p,r) = p\bar{T}(p,r) - T(0,r) - f_T(p) \tag{3.2}$$

with the boundary conditions,

(3.3) $$\nabla\bar{\rho}(R,p) = \nabla\bar{T}(R,p) = 0$$

(3.4) $$\bar{\rho}(a,p) = b\bar{T}(a,p) + c/p$$

(3.5) $$p\bar{T}(a,p) - T(0,a) = \alpha\nabla\bar{\rho}(a,p) + \beta\nabla\bar{T}(a,p)$$

where, $$L\frac{\partial T}{\partial t} = p\bar{T} - T(0,r)$$

and, $$L\frac{\partial \rho}{\partial t} = p\bar{\rho} - \rho(0,r) .$$

For T(0,r) take:

$$T(0,r) = T_o + T'(0,r)$$

where,

$$T_o = \lim_{+r \to a} T(0,r)$$

etc. for $\rho(0,r)$.

Explicit introduction of T_o will put the solution in a form that will reduce unequivocally to the initial condition discussed on page 21.

The heat diffusion equation with $\bar{T} = \bar{\Psi}_T/r$ becomes:

$$\frac{k}{r}\frac{d^2\bar{\Psi}_T}{dr^2} - p\frac{\bar{\Psi}_T}{r} = -\frac{\Psi_T(0,r)}{r} - f_T(p)$$

Let, $$\bar{\Psi}_T = \bar{\Psi}_h + \bar{\Psi}_1 + \bar{\Psi}_2$$

where $\bar{\psi}_h$ is the homogeneous solution, and $\bar{\psi}_1$, and $\bar{\psi}_2$ are particular solutions. With the boundary condition (3.3) included, one obtains for the homogeneous solution:

$$\bar{\psi}_h = A'(p) \sinh\left[\sqrt{\frac{p}{k}}(R-r) - \tanh^{-1} R\sqrt{\frac{p}{k}}\right]$$

and for the first particular solution:

$$\bar{\psi}_1 = (f_T + T_o)\frac{r}{p}$$

For $\bar{\psi}_2$ take:

$$\bar{\psi}_2 = \psi_2^o + f = \sum_m a'_m(p) \sin\frac{m\pi}{R-a}(r-a) + f$$

where $\bar{\psi}_2^o$ is imagined to be extended as an odd function, and f is a solution to,

$$\left(\frac{d^2}{dr^2} - \frac{p}{k}\right) f = 0$$

Substitution of $\bar{\psi}_2^o$ into

$$\frac{d^2\bar{\psi}}{dr^2} - \frac{p}{k}\bar{\psi} = -\frac{\psi'(0,r)}{k}$$

gives,

$$a'_m(p) = \frac{2/(R-a)}{k\left(\frac{m\pi}{R-a}\right)^2 + p}\int_a^R r\,T'(0,r)\sin\frac{m\pi}{R-a}(r-a)\,dr$$

The condition (3.3) is satisfied if:

$$\frac{d}{dr}\left[\frac{1}{r}\sum_m a'_m(p)\sin\frac{m\pi}{R-a}(r-a)\right]_{r=R} + \left[\frac{d}{dr}\left(\frac{f}{r}\right)\right]_{r=R} = 0$$

Take for f :

$$f = C_k(p)\,a'(p)\sinh\sqrt{\frac{p}{k}}\,(r-a)$$

$$\left[\frac{d}{dr}\left(\frac{f}{r}\right)\right]_{r=R} = \frac{C_k(p)\,a'(p)}{R}\left[\sqrt{\frac{p}{k}}\cosh\sqrt{\frac{p}{k}}\,(R-a) - \frac{1}{R}\sinh\sqrt{\frac{p}{k}}\,(R-a)\right]$$

$$\frac{d}{dr}\left[\frac{1}{r}\sum_m a'_m(p)\sin\frac{m\pi}{R-a}(r-a)\right]_{r=R} = \frac{\pi}{R(R-a)}\sum_m a'_m(p)\,m(-1)^m$$

$$\therefore\ C_k(p)\,a'(p) = \frac{\frac{\pi}{R-a}\sum_m a'_m(p)\,m(-1)^m}{\frac{1}{R}\sinh\sqrt{\frac{p}{k}}\,(R-a) - \sqrt{\frac{p}{k}}\cosh\sqrt{\frac{p}{k}}\,(R-a)}$$

$$a'(p) = \frac{\pi}{R-a}\sum_m m\,a'_m(p)\,(-1)^m$$

$$f = \frac{\pi}{R-a}\,\frac{\sum_m a'_m(p)\,m(-1)^m}{\frac{1}{R} - \sqrt{\frac{p}{k}}\coth\sqrt{\frac{p}{k}}\,(R-a)}\cdot\frac{\sinh\sqrt{\frac{p}{k}}\,(r-a)}{\sinh\sqrt{\frac{p}{k}}\,(R-a)}$$

Collecting results, the transformed solutions may be written:

$$\text{(3.6)}\qquad \overline{T} = \frac{A'(p)}{r}\sinh\left[\sqrt{\frac{p}{k}}\,(R-r) - \tanh^{-1}R\sqrt{\frac{p}{k}}\right] + \frac{f_T}{p} + \frac{T_o}{p}$$

$$+\sum_m \frac{a'_m(p)}{r}\sin\frac{m\pi}{R-a}\,(r-a) + \frac{C_k(p)\,a'(p)}{r}\sinh\sqrt{\frac{p}{k}}\,(r-a)$$

$$(3.7)\qquad \bar{\rho} = \frac{A(p)}{r}\sinh\left[\sqrt{\frac{p}{D}}(R-r) - \tanh^{-1}R\sqrt{\frac{p}{D}}\right] + \frac{\beta\rho}{p} + \frac{\rho_0}{p}$$

$$+\frac{1}{r}\sum_m a_m(p)\sin\frac{m\pi}{R-a}(r-a) + \frac{C_D(p)\,q(p)}{r}\sinh\sqrt{\frac{p}{D}}(r-a)$$

where,

$$a'_m(p) = \frac{2/(R-a)}{k\left(\frac{m\pi}{R-a}\right)^2 + p}\int_a^R T'(0,r)\,r\sin\frac{m\pi}{R-a}(r-a)\,dr$$

$$a_m(p) = \frac{2/(R-a)}{D\left(\frac{m\pi}{R-a}\right)^2 + p}\int_a^R \rho'(0,r)\,r\sin\frac{m\pi}{R-a}(r-a)\,dr$$

$$q'(p)C_k(p) = \frac{\frac{\pi}{R-a}\sum_m a'_m(p)\,m(-1)^m}{\frac{1}{R}\sinh\sqrt{\frac{p}{k}}(R-a) - \sqrt{\frac{p}{k}}\cosh\sqrt{\frac{p}{k}}(R-a)}$$

and,

$$q(p)C_D(p) = \frac{\frac{\pi}{R-a}\sum_m a_m(p)\,m(-1)^m}{\frac{1}{R}\sinh\sqrt{\frac{p}{D}}(R-a) - \sqrt{\frac{p}{D}}\cosh\sqrt{\frac{p}{D}}(R-a)}$$

(3.6) and (3.7) can now be substituted into boundary conditions (3.4) and (3.5) in order to determine A(p) and A'(p). With the abbreviated functions:

$$\eta_k(r) = \sqrt{\frac{p}{k}}(R-r) - \tanh^{-1}R\sqrt{\frac{p}{k}}$$

$$\eta_D(r) = \sqrt{\frac{P}{D}}(R-r) - \tanh^{-1} R\sqrt{\frac{P}{D}}$$

the condition (3.4) is:

$$(3.8) \qquad \frac{A(P)}{a}\sinh\eta_D(a) - b\,\frac{A'(P)}{a}\sinh\eta_k(a) = h_1(P)$$

where,

$$h_1(P) = \frac{b f_T(P) - f_P(P)}{P} + \frac{c'}{P}$$

and,

$$c' = bT_0 + c - \rho_0 .$$

Boundary condition (3.5) becomes, after some rearrangement:

$$(3.9) \quad \frac{A}{P}\alpha\left[\sqrt{\frac{P}{D}}\cosh\eta_D(a) + \frac{\sinh\eta_D(a)}{a}\right] + \frac{A'}{a}\left\{\rho\sinh\eta_k(a) + \beta\left[\sqrt{\frac{P}{k}}\coth\eta_k(a) + \frac{\sinh\eta_k(a)}{a}\right]\right\}$$

$$= h_2(P)$$

where,

$$h_2(P) = (T_a - T_0) - f_T(P) + \frac{\alpha\pi}{a(R-a)}\sum_m m\,a_m(P) + \sqrt{\frac{P}{D}}\,\frac{\alpha\,Q(P)\,C_D(P)}{a}$$

$$+ \beta\,\frac{\pi}{a(R-a)}\sum_m a'_m(P)\,m + \sqrt{\frac{P}{k}}\,\frac{\beta\,C_k(P)\,Q'(P)}{a} .$$

Solving (3.8) and (3.9) for A(p) leads to:

$$(3.10)\quad \bar{\rho}(r,p)=\frac{a}{r}\,\frac{h_1(p)[p+\beta\chi_k(a)]+b\,h_2(p)}{p+\beta\chi_k(a)+ba\chi_D(a)}\cdot\frac{\sinh\eta_D(r)}{\sinh\eta_D(a)}+\frac{f_\rho(p)}{p}$$

$$+\frac{\rho_0}{p}+\frac{1}{r}\sum_m a_m(p)\sin\left[\frac{m\pi}{R-a}(r-a)\right]+\frac{\mathcal{Q}(p)\,C_D(p)}{r}\sinh\sqrt{\frac{p}{D}}(r-a)$$

and,

$$(3.11)\quad \bar{T}(r,p)=\frac{a}{r}\,\frac{h_2(p)-\alpha h_1(p)\chi_D(a)}{p+\beta\chi_k(a)+ba\chi_D(a)}\,\frac{\sinh\eta_k(r)}{\sinh\eta_k(a)}+\frac{f_T(p)}{p}+\frac{T_0}{p}$$

$$+\frac{1}{r}\sum_m a'_m(p)\sin\frac{m\pi}{R-a}(r-a)+\frac{\mathcal{Q}'(p)\,C_k(p)}{r}\sinh\sqrt{\frac{p}{k}}(r-a)$$

where,

$$\chi_D(r)=\sqrt{\frac{p}{D}}\coth\eta_D(r)+\frac{1}{r}$$

and,

$$\chi_k(r)=\sqrt{\frac{p}{k}}\coth\eta_k(r)+\frac{1}{r}\ .$$

Inversion of the Transformed Problem:

The problem is now reduced to one of inverting $\bar{T}$ and $\bar{\rho}$, which is to be attempted by using the inversion integral[34]. While the justification for the validity of the

above solutions will be sought on physical grounds, that is by demonstrating the physical reasonableness of the solution in terms of its initial and boundary behavior, some mathematical facets of the solutions should here be pointed out.

First, despite the ubiquity of square-root terms, the solutions have no branch points.[35] This is most easily seen by noting that an expansion of the sinh terms around $p = 0$ will not produce a branch point (at $p = 0$) if this expansion is either divided or multiplied by $p^{1/2}$. Inspection of (3.10) and (3.11) reveals that there are exactly enough such terms to be paired to every sinh term.

Second, in the contour relating to the inversion integral (shown), the contribution to the integral around ABCD vanishes as $\rho \to \infty$, where $p = \rho e^{i\theta}$. This is shown in Appendix I.

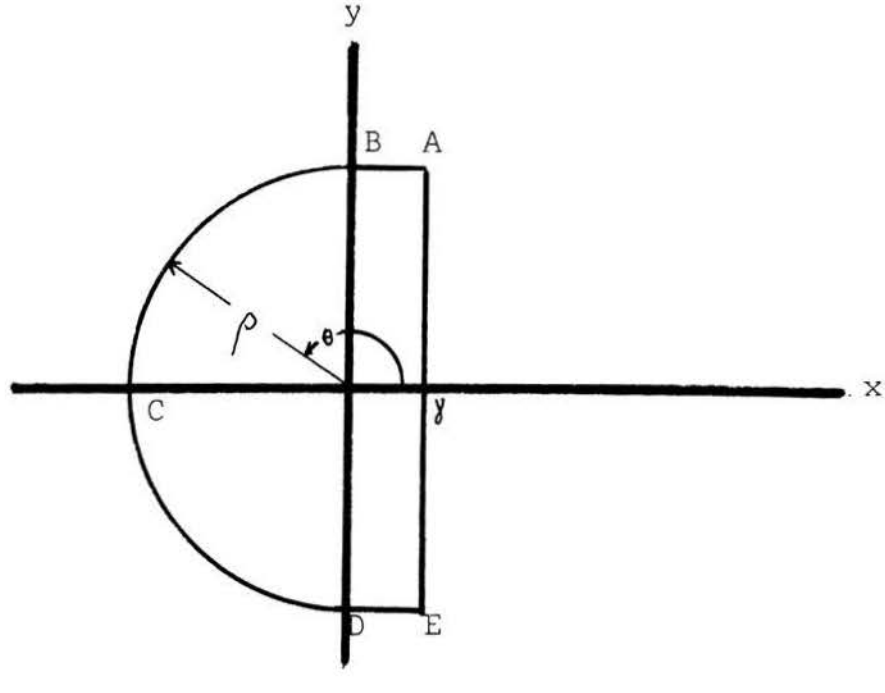

Figure 2. Inversion Integral Contour

The inversion integral is:

$$L^{-1}f(p) = \frac{1}{2\pi i}\lim_{\rho\to\infty}\int_{\gamma-i\rho}^{\gamma+i\rho} f(p)e^{pt}dp.$$

Here γ divides the complex plane into a right-hand region which is free of poles and a left-hand region which is not. The existence of γ is due to a theorem quoted by Scott.[36]

Finally it is argued in Appendix II (ultimately with the help of a plot in the complex plane) that all singularities occur along the non-positive real axis, and are given by the roots of:

$$g(p) = p + \beta\chi_k(a) + ba\chi_D(a). \tag{3.12}$$

These will be denoted by p_ℓ, $\ell = 1, 2, \ldots$

Before performing the inversions, some abbreviated functions which are to be used will be collected here.

$$\eta_D(r) = \sqrt{\frac{p}{D}}(R-r) - \tanh^{-1}R\sqrt{\frac{p}{D}}$$

$$\eta_k(r) = \sqrt{\frac{p}{k}}(R-r) - \tanh^{-1}R\sqrt{\frac{p}{k}}$$

$$\chi_D(r) = \sqrt{\frac{p}{D}}\coth\eta_D(r) + \frac{1}{r}$$

$$\chi_k(r) = \sqrt{\frac{p}{k}}\coth\eta_k(r) + \frac{1}{r}$$

$$g(p) = p + \beta\chi_k(a) + ba\chi_D(a)$$

$$\mathfrak{Z}_D(r) = \frac{a}{r}\, g^{-1}(p)\, \frac{\sinh \eta_D(r)}{\sinh \eta_D(a)}$$

$$\mathfrak{Z}_k(r) = \frac{a}{r}\, g^{-1}(p)\, \frac{\sinh \eta_k(r)}{\sinh \eta_k(a)}$$

$$D_m = D\left(\frac{m\pi}{R-a}\right)^2$$

$$k_m = k\left(\frac{m\pi}{R-a}\right)^2$$

$$a(p) = \frac{\pi}{R-a} \sum_m m\, a_m(p)\, (-1)^m$$

$$a'(p) = \frac{\pi}{R-a} \sum_m m\, a_m'(p)\, (-1)^m$$

$$c_D(p) = \left\{ \frac{1}{R} \sinh \sqrt{\frac{p}{D}}(R-a) - \sqrt{\frac{p}{D}} \cosh \sqrt{\frac{p}{D}}(R-a) \right\}^{-1}$$

$$c_k(p) = \left\{ \frac{1}{R} \sinh \sqrt{\frac{p}{k}}(R-a) - \sqrt{\frac{p}{k}} \cosh \sqrt{\frac{p}{k}}(R-a) \right\}^{-1}$$

$$h_1(p) = \frac{1}{P}\left[\oint_\rho(p) - b\oint_T(p) + c'\right]$$

$$h_2(p) = (T_a - T_o) - \oint_T(p) + \frac{\alpha\pi}{a(R-a)}\sum_m m\, a_m(p) + \sqrt{\frac{P}{D}}\,\frac{a\,\mathcal{Q}(p)\,C_D(p)}{a}$$

$$+\frac{\beta\pi}{a(R-a)}\sum_m m\, a_m'(p) + \sqrt{\frac{P}{k}}\,\frac{\beta\, C_k(p)\,\mathcal{Q}'(p)}{a}.$$

Since convolution techniques are to be enlisted in the inversion of ρ and $\bar{T}$, the important individual transforms of the above functions will also be collected. To do this straight-forward summation of residues will be employed, following the techniques outlined in Scott.[38] The poles are assumed single.[39]

$$L^{-1}\Xi_D(r) = \sum_\ell \bar{\Xi}_D(p_\ell, r)\, e^{p_\ell t} \tag{3.15}$$

where

$$\bar{\Xi}_D(r,p) = \frac{a}{r}\left(\frac{dg}{dp}\right)^{-1}\frac{\sinh \eta_D(r)}{\sinh \eta_D(a)}$$

Similarly,

$$L^{-1}\chi_k(a)\Xi_D(r) = \sum_\ell X_k\,\bar{\Xi}_D(p_\ell, r)\, e^{p_\ell t} \tag{3.16}$$

where,

$$X_{ik} = \chi_D(p_\ell)$$

(3.17) $$L^{-1}h_1(p) = L^{-1}(f_p - b f_T) + c'$$

In order to determine $L^{-1}h_2(p)$ it is necessary to find,

$$L^{-1}a'(p)\,C_k(p)\sqrt{\frac{p}{k}} = \frac{\pi}{R-a}\,L^{-1}\sum a'_m(p)\,m(-1)^m * L^{-1}\frac{\sqrt{\frac{p}{k}}}{\frac{1}{R}\sinh\sqrt{\frac{p}{k}}(R-a)-\sqrt{\frac{p}{k}}\cosh\sqrt{\frac{p}{k}}(R-a)}$$

where the symbol $*$ represents convolution. The transform:

$$L^{-1}\frac{\sqrt{\frac{p}{k}}}{\frac{1}{R}\sinh\sqrt{\frac{p}{k}}(R-a)-\sqrt{\frac{p}{k}}\cosh\sqrt{\frac{p}{k}}(R-a)}$$

can be performed by summation of residues around the contour ABCD shown in Figure 2.

$$L^{-1}\sqrt{\frac{p}{k}}\,C_k(p) = -2\sum_j \frac{\sqrt{\frac{p_j}{k}}\,e^{p_j t}}{\frac{1}{\sqrt{p_j k}}\left[\frac{a}{R}\cosh\sqrt{\frac{p_j}{k}}(R-a)+(R-a)\sqrt{\frac{p_j}{k}}\sinh\sqrt{\frac{p_j}{k}}(R-a)\right]}$$

where the p_j's are solutions to:

$$\sinh\sqrt{\frac{p}{k}}(R-a) = R\sqrt{\frac{p}{k}}\cosh\sqrt{\frac{p}{k}}(R-a).$$

The other inversion is:

$$L^{-1}a'_m(p) = e^{-k_m t}\,\frac{2}{R-a}\int_a^R T'(0,r)\,r\sin\frac{m\pi}{R-a}(r-a)\,dr.$$

Performing the convolution gives:

$$L^{-1}\mathcal{Q}'(p)C_k(p)\sqrt{\frac{p}{k}} = \sum_{j,m} A'_m C_k(p_j)\sqrt{\frac{p_j}{k}} \quad \frac{e^{p_j t} - e^{-k_m t}}{p_j + k_m}$$

where,

$$A'_m = \frac{2}{R-a}\int_a^R T'(0,r)\, r \sin\frac{m\pi}{R-a}(r-a)\, dr$$

and,

$$C_k(p_j) = \frac{2\sqrt{p_j k}}{\frac{a}{R}\cosh\sqrt{\frac{p_j}{k}}(R-a) + (R-a)\sqrt{\frac{p_j}{k}}\sinh\sqrt{\frac{p_j}{k}}(R-a)}.$$

Likewise,

$$L^{-1}\mathcal{Q}(p)C_D(p)\sqrt{\frac{p}{D}} = \sum_m A_m C_D(p_j)\sqrt{\frac{p_j}{D}}\ \frac{e^{p_j t} - e^{-D_m t}}{p_j + D_m}.$$

This gives for $L^{-1}h_2(p)$:

$$L^{-1}h_2(p) = (T_a - T_o)\delta(t) - F_T(t) + \frac{a\pi}{a(R-a)}\sum_m A_m m e^{-D_m t}$$

$$\frac{+\beta\pi}{a(R-a)}\sum_m A'_m m e^{-k_m t} + \frac{\alpha}{a}\sum_m A_m C_D(p_j)\sqrt{\frac{p_j}{D}}\ \frac{e^{p_j t} - e^{-D_m t}}{p_j + D_m}$$

$$+ \frac{\beta}{a}\sum_m A'_m C_k(p_j)\sqrt{\frac{p_j}{k}}\ \frac{e^{p_j t} - e^{-k_m t}}{p_j + k_m}$$

where $\delta(t)$ is the Dirac Delta function.

Inversion of $\bar{T}(p,r)$:

The inversion of $\bar{T}(p,r)$ may now be written in terms of convolutions of the inverses calculated above.

$$\bar{T}(p,r) = h_2(p)\,\bar{\Xi}_K(r) - \alpha h_1(p)\,\bar{\Xi}_K(r)\,\chi_D(a) + \frac{f_T(p)}{p} + T_0/p$$

$$+ \frac{1}{r}\sum_m a_m'(p)\sin\frac{n\pi}{R-a}(r-a) + \frac{\mathcal{Q}'(p)C_K(p)}{r}\sinh\sqrt{\frac{p}{k}}(R-a)$$

$$L^{-1}h_2(p)\,\bar{\Xi}_K(r) = (T_a - T_0)\sum_\ell \bar{\bar{\Xi}}_K(p_\ell, r)\,e^{p_\ell t} - \sum_\ell \bar{\bar{\Xi}}_K(p_\ell, r)\,F_T(t) *_\ell e^{p_\ell t}$$

$$+ \frac{\alpha\pi}{a(R-a)}\sum_{m,\ell} m A_m\,\bar{\bar{\Xi}}_K(p_\ell, r)\,\frac{e^{p_\ell t} - e^{-D_m t}}{p_\ell + D_m}$$

$$+ \frac{\beta\pi}{a(R-a)}\sum_{m,\ell} m A_m'\,\bar{\bar{\Xi}}_K(p_\ell, r)\,\frac{e^{p_\ell t} - e^{-k_m t}}{p_\ell + k_m}$$

$$+ \frac{\alpha}{a}\sum_{m,j,\ell} \frac{A_m C_D(p_j)}{p_j + D_m}\,\bar{\bar{\Xi}}_K(p_\ell, r)\left[\frac{e^{p_j t} - e^{-D_m t}}{p_j - p_\ell} - \frac{e^{p_\ell t} - e^{-D_m t}}{p_\ell + D_m}\right]$$

$$+ \frac{\beta}{a}\sum_{m,j,\ell} \frac{A_m' C_K(p_j)}{p_j + k_m}\,\bar{\bar{\Xi}}_K(p_\ell, r)\left[\frac{e^{p_j t} - e^{p_\ell t}}{p_j - p_\ell} - \frac{e^{p_\ell t} - e^{-D_m t}}{p_\ell + D_m}\right].$$

$$(3.19)\quad L^{-1}\, h_1(p)\, \Xi_k(r)\, X_D(a) = L^{-1}(bF_T - F_p) * \left[\Xi_k(0) X_D(0) + \sum_\ell \frac{\Xi_k(\rho_\ell, r) X_D \ell^{\rho_\ell t}}{\rho_\ell} \right]$$

$$+ C' \left[\Xi_k(0) X_D(0) + \sum_\ell \frac{\Xi_k(\rho_\ell, r) X_D}{\rho_\ell} \ell^{\rho_\ell t} \right]$$

where

$$\Xi_k(0)\, X_D(0) = \lim_{p \to 0} \Xi_k(r)\, X_D(a).$$

The remaining inversions have already been calculated. Collecting terms, we can now write the solution for the temperature as a function of r and t.

(3.20)

$$T(r,t) = (T_a - T_o) \sum_\ell \Xi_k(\rho_\ell, t) \ell^{\rho_\ell t} - \sum_\ell \Xi_k(\rho_\ell, r)\, F_T(t) * \ell^{\rho_\ell t}$$

$$+ \frac{\alpha \pi}{a(R-a)} \sum_{m,\ell} m A_m \Xi_k(\rho_\ell, r) \frac{\ell^{\rho_\ell t} - \ell^{-D_m t}}{\rho_\ell + D_m} + \frac{\beta \pi}{a(R-a)} \sum_{m,\ell} m A'_m \Xi_k(\rho_\ell, r) \frac{\ell^{\rho_\ell t} - \ell^{-k_m t}}{\rho_\ell + k_m}$$

$$+ \frac{\alpha}{a} \sum_{m,j,\ell} \frac{A_m C_D(\rho_j)}{\rho_j + D_m} \sqrt{\frac{\rho_j}{D}}\, \Xi_k(\rho_\ell, r) \left[\frac{\ell^{\rho_j t} - \ell^{\rho_\ell t}}{\rho_j - \rho_\ell} - \frac{\ell^{\rho_\ell t} - \ell^{-D_m t}}{\rho_\ell + D_m} \right]$$

$$+ \frac{\beta}{a} \sum_{m,j,\ell} \frac{A'_m C_K(\rho_j)}{\rho_j + k_m} \sqrt{\frac{\rho_j}{k}}\, \Xi_k(\rho_\ell, r) \left[\frac{\ell^{\rho_j t} - \ell^{\rho_\ell t}}{\rho_j - \rho_\ell} - \frac{\ell^{\rho_\ell t} - \ell^{-k_m t}}{\rho_\ell + k_m} \right]$$

$$- \bar{\Xi}_K(0)\bar{X}_D(0)\alpha\int_0^t (bF_T - F_\rho)\,dt - L_1^{-1}(bF_T - F_\rho) * \sum_\ell \bar{\Xi}_K(p_\ell, r)\bar{X}_D \frac{e^{p_\ell t}}{p_\ell}$$

$$- \alpha c' \bar{\Xi}_K(0)\bar{X}_D(0) - \alpha c' \sum_\ell \bar{\Xi}_K(p_\ell, r) X_D \frac{e^{p_\ell t}}{p_\ell} + T_o + \int_0^t F_T(t)\,dt$$

$$+ \frac{1}{r}\sum_m A_m' e^{-k_m t} \sin\frac{m\pi}{R-a}(r-a) + \frac{1}{r}\sum_{m,j} A_m' C_K(p_j)\frac{e^{p_j t} - e^{-k_m t}}{p_j + k_m} \sinh\sqrt{\frac{p_j}{k}}(r-a).$$

Inversion of $\bar{\rho}(p,r)$:

The inversion of $\bar{\rho}(p,r)$ proceeds much like that of $\bar{T}(p,r)$.

$$(3.21)\quad \rho(r,t) = c'\sum_\ell \bar{\Xi}_D(r,t) e^{p_\ell t} + L^{-1}(bf_T - f_\rho) * \sum_\ell \bar{\Xi}_D(p_\ell, r) e^{p_\ell t}$$

$$+\beta L^{-1}(bf_T - f_\rho) * \left[\bar{\Xi}_D(0)\bar{X}_K(0) + \sum_\ell \bar{\Xi}_D(p_\ell, r)\bar{X}_K \frac{e^{p_\ell t}}{p_\ell}\right]$$

$$+\beta c'\left[\bar{\Xi}_D(0)X_K(0) + \sum_\ell \bar{\Xi}_D(p_\ell, r)X_K \frac{e^{p_\ell t}}{p_\ell}\right]$$

$$+b(T_a-T_o)\sum_{\ell}\bar{\bar{\Xi}}_D(\rho_\ell,r)\,e^{\rho_\ell t}-b\sum_{\ell}\bar{\bar{\Xi}}_D(\rho_\ell,r)\,F_T(t)*e^{\rho_\ell t}$$

$$+\frac{\alpha\pi b}{a(R-a)}\sum_{m,\ell}m A_m\,\bar{\bar{\Xi}}_D(\rho_\ell,r)\,\frac{e^{\rho_\ell t}-e^{-D_m t}}{\rho_\ell+D_m}+\frac{\beta\pi b}{a(R-a)}\sum_{m,\ell}m A'_m\,\bar{\bar{\Xi}}_D(\rho_\ell,r)\,\frac{e^{\rho_\ell t}-e^{-k_m t}}{\rho_\ell+k_m}$$

$$+\frac{\alpha b}{a}\sum_{m,j,\ell}\frac{A_m C_D(\rho_j)}{\rho_j+D_m}\sqrt{\frac{\rho_j}{D}}\left[\frac{e^{\rho_j t}-e^{\rho_\ell t}}{\rho_j-\rho_\ell}-\frac{e^{\rho_\ell t}-e^{-D_m t}}{\rho_\ell+D_m}\right]\bar{\bar{\Xi}}_D(\rho_\ell,r)$$

$$+\frac{\beta b}{a}\sum_{m,j,\ell}\frac{A'_m C_k(\rho_j)}{\rho_j+k_m}\sqrt{\frac{\rho_j}{k_m}}\left[\frac{e^{\rho_j t}-e^{\rho_\ell t}}{\rho_j-\rho_\ell}-\frac{e^{\rho_\ell t}-e^{-k_m t}}{\rho_\ell+k_m}\right]\bar{\bar{\Xi}}_D(\rho_\ell,r)+\rho_o$$

$$+\int_0^t F_\rho(t)\,dt+\frac{1}{r}\sum_m A_m\sin\frac{m\pi}{R-a}(r-a)+\sum_{m,j}\frac{A_m C_D(\rho_j)}{r}\sinh\sqrt{\frac{\rho_j}{D}}(r-a).$$

The solutions are in terms of convolutions with $F_T(t)$ and $F_\rho(t)$. These convolutions are easy to calculate if the form of $F_T(t)$ and $F_\rho(t)$ are assumed to be parabolic, as in Appendix IV.

$$(3.22)\qquad F_T(t)*e^{\rho_\ell t}=\frac{2\Gamma_T}{\rho_\ell^2}\left[e^{\rho_\ell t}-\rho_\ell t-1\right]-\frac{\Gamma_T\,\Delta t}{\rho_\ell}\left(e^{\rho_\ell t}-1\right)$$

The two equations (3.20) and (3.21) represent the solution of the double diffusion problem cast into fairly general form. The length of these solutions makes numerical evaluation rather difficult. In the next chapter numerical results will be obtained for a simplified problem with $F_T = F_\rho = 0$.

CHAPTER IV

The solution derived in the foregoing chapter can be shortened by simplifying the physical situation it represents. It will be seen that such simplification will yield a solution which can still provide much of the information desired, as well as a reasonably convincing argument for the correctness of the mathematics. In this chapter, therefore, we are concerned with numerical solutions pertaining to a simpler problem. Before developing these solutions it is necessary to discuss some intermediate steps which are common to all forms of $T(r,t)$ and $\rho(r,t)$.

Preliminary Steps:

First the transcendental equation must be solved, since any solution involves at least one sum over these roots. From Appendix II, the roots are expected to be real and negative. The substitution,

$$\sqrt{P} = i\nu$$

gives

$$q(i\nu) = \frac{C_o - \nu^2}{\nu} + A_o \cot(a_o\nu - \tan^{-1} a_o'\nu) + B_o \cot(b_o\nu - \tan^{-1} b_o'\nu)$$

where,

$$C_o = \beta + b\alpha \qquad a_o = (R-a)/\sqrt{k} \qquad b_o' = R/\sqrt{D}$$

$$A_o = \beta/\sqrt{k} \qquad b_o = (R-a)/\sqrt{D}$$

$$B_o = b\alpha/\sqrt{D} \qquad a_o' = R/\sqrt{k}$$

The roots of this equation are calculable by means of a computer program presented in Appendix V. The smallest root is calculated with extra accuracy, and there is a special root, calculated separately in the program, near $\sqrt{C_o}$; otherwise the roots are rather close to the infinite discontinuities given by:

$$\cot(b_o\nu - \tan^{-1} b_o'\nu) = 0$$

and,

$$\cot(a_o\nu - \tan^{-1} a_o'\nu) = 0.$$

The computer program is based on these values of v as first approximations to the actual roots.

Second, the writer has found it helpful to put the expressions Ξ_D, Ξ_k, X_D, and X_k in forms into which one can explicitly substitute $|p_1|$. The evaluation of these follows:

$$X_k(|p_1|, r) = \frac{1}{r} + \sqrt{\frac{|p_1|}{k}}\cot\left[\sqrt{\frac{|p_1|}{k}}(R-r) - \tan^{-1}\sqrt{\frac{|p_1|}{k}}R\right] \tag{4.1}$$

$$\Xi_k(|p_1|, r) = \frac{\frac{a}{r}\,\frac{\sin\left[\sqrt{\frac{|p_1|}{k}}(R-r) - \tan^{-1}R\sqrt{\frac{|p_1|}{k}}\right]}{\sin\left[\sqrt{\frac{|p_1|}{k}}(R-a) - \tan^{-1}R\sqrt{\frac{|p_1|}{k}}\right]}}{1 + \beta\left\{-\frac{\cot\sqrt{\frac{|p_1|}{k}}(R-a) - \tan^{-1}R\sqrt{\frac{|p_1|}{k}}}{2\sqrt{|p_1|k}} + \left[R - a - \frac{R}{1+R^2\frac{|p_1|}{k}}\right]\frac{\csc^2\left[\sqrt{\frac{|p_1|}{k}}(R-a) - \tan^{-1}R\sqrt{\frac{|p_1|}{k}}\right]}{2k}\right\}} \tag{4.2}$$

$$+ b\alpha\left\{-\frac{\cot\left[\sqrt{\frac{|p_1|}{D}}(R-a) - \tan^{-1}R\sqrt{\frac{|p_1|}{D}}\right]}{2\sqrt{|p_1|D}} + \left[R - a - \frac{R}{1+R^2\frac{|p_1|}{D}}\right]\frac{\csc^2\left[\sqrt{\frac{|p_1|}{D}}(R-a) - \tan^{-1}R\sqrt{\frac{|p_1|}{D}}\right]}{2D}\right\}$$

Analogous expressions are obtained for $\overline{\overline{\Xi}}_D(r,\rho_\ell)$ and $\overline{\overline{X}}_D$.

Third, a mass influx calculation will be needed. For this we will use:

$$\Delta m(t) = 4\pi a^2 D \int_0^t \nabla\rho(r,t)\Big|_{r=a} dt \tag{4.3}$$

where $\Delta m(t)$ is the mass incremented in a time t. The calculation of $\Delta m(t)$ is simplified by the identity,

$$\frac{d}{dr}\,\overline{\overline{\Xi}}_D(\rho_\ell,r) = -\overline{\overline{X}}_D(\rho_\ell,r)\,\overline{\overline{\Xi}}_D(\rho_\ell,r)$$

Finally, the calculations will be compared with quasi steady-state calculations which are solutions to the equations:

$$\nabla^2\rho_{ss} = \nabla^2 T_{ss} = 0.$$

At each time t, one puts:

$$\rho_{ss}(a) = \rho(t,a)$$

$$\rho_{ss}(R) = \rho(t,R)$$

$$T_{ss}(a) = T(t,a)$$

$$T_{ss}(R) = T(t,R).$$

The right-hand values are those calculated from the correct, fixed radius, solutions. We can analyze the quasi steady-

state approximation according to the following argument. The fixed boundary solution permits the calculation of a "virtual" mass influx, that is, the influx which occurs when the drop radius does not grow into the surrounding atmosphere. The difference between this and the true mass influx will have to be considered small compared with either influx term. Also the mass of the drop, throughout its brief "growth" period, is considered constant, so that its contribution to the specific heat of the drop is necessarily neglected. However an averaged mass, somewhere between initial and final masses for a given growth period t, could be introduced as an approximation. The radial change is given by,

$$\frac{\Delta a}{a_o} = \frac{1}{3} \frac{\Delta m}{m_o}$$

where subscript zero denotes initial values. Now the validity of an appraisal of a steady-state approximation will depend on the condition that the variation of the steady-state solution with respect to the above change in radius be negligible. The validity of the steady-state approximation then depends on the magnitude of its departure from the fixed radius solution.

Numerical Solutions:

The simplest physical problem to which the solution applies is that of a drop suddenly inserted into an atmosphere of constant supersaturation, where the drop is initially at the same temperature as the atmosphere. For these

conditions the boundary conditions give simply:

$$h_1(p) = c'/p$$

and,

$$h_2(p) = 0$$

where,

$$c' = bT_o - \rho_o + c$$

and where T_o and ρ_o are the initial temperature and vapor density respectively. In this case the transformed solutions reduce to:

$$\bar{T} = -\frac{\alpha c'}{p} \bar{\Xi}_k(p,r) \bar{X}_D(a) + T_o/p \tag{4.4}$$

$$\bar{\rho} = \frac{c'}{p}(p+\beta\chi_k)\bar{\Xi}_D(p,r) + \rho_o/p \tag{4.5}$$

which have the inversions:

$$T(r,t) = -\alpha c' \bar{\Xi}_k(0)\bar{X}_D(0) - \alpha c' \sum_\ell \bar{\Xi}_k(p_\ell,r)\bar{X}_D\, e^{-|p_\ell|t} + T_o \tag{4.6}$$

$$\rho(r,t) = c' \lim_{p\to 0}\left[p+\chi_k(a)\right]\bar{\Xi}_D(r,p) + c' \sum_\ell \frac{p_\ell+\beta\bar{X}_k}{p_\ell}\bar{\Xi}_D(p_\ell,r)\, e^{-|p_\ell|t} + \rho_o \tag{4.7}$$

where, if a << R, as will usually be the case,

$$\bar{\Xi}_k(0)\bar{X}_D(0) \cong \frac{\alpha c'/D}{\beta/k + b\alpha/D}$$

and,

$$\lim_{p\to 0}\left[p+\chi_k(a)\right]\bar{\Xi}_D(r,p) = \frac{\beta/k}{\beta/k + b\alpha/D}.$$

In these solutions a constant steady-state temperature and density would finally ensue given by:

$T_0 - \alpha c' \Xi_K(0) X_D(0)$, and $\rho_0 - c' \lim_{p \to 0} \left[p + \chi_K(a) \right] \Xi_D(p,r)$,

that is at a value of T higher than T_0 and a value of ρ lower than ρ_0. This fact, which is physically obvious, is attributable to the sign of c'. For growth, equilibrium must be violated in such a way that ρ_0 is greater than its equilibrium value. Of course the validity of the fixed radius solution is destroyed long before true steady-state is ever reached. Our interest is in the rapidly established quasi steady-state solution.

The sample problem to be considered first, while not directly applicable to the problem posed at the outset of this study, will serve to lend plausibility to the solutions obtained, and perhaps have some bearing on the "quenching effect" of aerosol particles discussed by Riess and La Mer.[40] Data for a typical light expansion were obtained from Grayson.[41] These are as follows:

Supersaturation (S) = 5.89

Initial temperature (T_0) = -3.6°C

Initial vapor density (ρ_0) = 17.76 x 10^{-6} gms/cm.^{3}

Number of drops per cm^3 (N) = 8

Radius of drop (a) = .001 cm.

Radius of impermeable sphere (R) = .3 cm.

The cloud-chamber gas is composed of Helium as a solvent and water vapor as a dilute solute. Experimental values for D,

the vapor diffusion coefficient, were found in an article by Schwerz and Brow,[42] and extrapolated down to the temperature of interest. The diffusivity was calculated for Helium alone, following Bagge, Bekow, and Becker,[43] from data available in the International Critical Tables.[44] Vapor equilibrium parameters were taken from Buecher's Thesis.[45] Supersaturation curves corresponding to temperature and density solutions are easily computed from the definition:

$$S = \frac{\text{actual vapor density at temperature T}}{\text{equilibrium vapor density at temperature T}}.$$

In Appendix VII a sample computer program is displayed for the evaluation of the temperature. This is simply equation (4.6) with (4.1) and (4.2) directly substituted. The programs for density and mass influx are similar. Solutions to the 10 micron drop problem, with drop temperature equal to the initial ambient temperature, are displayed in Figures 3, 4, 7 and 8, for two times, $t = 10^{-4}$ seconds and $t = 10^{-3}$ seconds. Also shown, for the same times, are the supersaturation curves (calculated from Becker-Doring[46] theory) in Figures 5, 6, 9 and 10 respectively. Each figure shows both the fixed radius solution and the quasi steady-state solution (provided they differ noticeably). The difference between quasi steady-state nucleation rate profiles and those for the fixed radius problem is surprisingly large when compared with the corresponding difference in supersaturations. This difference is due to the high sensitivity of the nucleation rate formulae to supersaturations above critical, and

leads to a significant disparity, in the values for dead space volumes, which lingers on up to 10^{-3} seconds when steady-state and fixed radius solutions are nearly concurrent. Mass influx calculations give, after 10^{-3} seconds,

$$\frac{\Delta m}{m_o} = .047$$

which leads to less than a 2% change in radius, giving no detectable change in steady-state solutions. The present analysis appears to indicate that the growth of a 10 micron drop is entirely described by the fixed radius theory in conjunction with the quasi steady-state theory, and in addition that the quasi steady-state theory holds for a large duration of the growth time. Additional graphs, for the same 10 micron drop problem, but now with an initial temperature of -.1°C (where T_o = -3.6°C) are shown in Figures 11 and 12. The -.1° is obtained from Beucher's treatment.[47] In each of the calculations it is easy to check that the condition

$$\rho(a,t) = bT(a,t) + c$$

is satisfied, and that:

$$\rho(R,t) = \rho_o \quad \text{and} \quad T(R,t) = T_o .$$

Furthermore, if the series solution is carried out far enough, the initial conditions emerge as time goes to zero.

Additional solutions, along with pertinent data, are shown in Figures 13 and 14 for 1 micron drop radius. Quasi

steady-state represents a good approximation in less than 10^{-4} seconds. At this time,

$$\frac{\Delta m}{m_o} = .18$$

and

$$\frac{\Delta a}{a_o} = .06.$$

Now, while a 6% change in radius yields again an undetectable change in the quasi steady-state solution, an 18% change in mass should lead to a protraction of the time it takes the fixed radius solution to concur with the quasi steady-state solution. If the drop is endowed with a slightly greater mass, say about midway between initial and final masses for t = 10^{-4} seconds, a certain "sluggishness" should be observed. Despite this, Figures 15 and 16 show that the quasi steady-state solution is still reached before 10^{-4} seconds. It should be mentioned that at and below one micron the usual macroscopic theory begins to lose significance, since λ, the mean free path, is of the order of 10^{-5} cm. for present conditions.

In spite of the above reservations it is interesting to repeat the computations for a .5 micron drop. Table I shows an analysis of the fixed radius solutions for 10^{-5} seconds, 2×10^{-5} seconds, and 5×10^{-5} seconds along with steady state solutions evaluated at the original radius of the drop, and at the radius it would have (if growth were possible) at t = 2×10^{-5} seconds. Again, an averaged mass is obtained by introducing an effective density of water.

In 10^{-5} seconds the largest departure of the fixed radius solution form the quasi steady-state solution is .36%. During this time mass influx is 8% and radial growth about 3%. The situation has not changed much in 2×10^{-5} seconds, except that the mass influx becomes large enough, at this point, to show a perceptible departure of the steady-state solution calculated by using the incremented radius, from the steady-state solution calculated by using the original radius. This departure is still somewhat less, however, than that between the fixed radius solution and the steady-state solution.

Assuming the validity of the fixed radius solution to extend to 2×10^{-5} seconds, the maximum departure from steady-state, at 2×10^{-5} seconds is less than .3% (although it should be mentioned that the forth place in vapor and temperature calculations is somewhat questionable due to the fact that the series solutions necessarily carry only a finite number of terms).

Quasi Steady-State Results:

The above results appear to support an entirely steady-state computation "starting", let us say, the droplet at .5 microns. The results of such a calculation are shown in Figures 15 and 16. It is hard to say precisely what error is incurred by assuming that the droplet attains a size of .5 microns "instantaneously"; however the results of simply extending quasi steady-state theory to a = 0 put this time at an order of magnitude of 10^{-4} seconds.

Extension to Higher Supersaturations:

The approximate validity of a quasi steady-state approach to the evaluation of dead space has been suggested, of course, only for the set of data presented on page 45. For higher supersaturations one expects the validity of the fixed radius solution to be more short-lived, while departures of transient terms from steady-state solutions become larger. In short, the ultimate breakdown of the quasi steady-state approximation is anticipated as supersaturations are increased. Now we can increase supersaturations simply by increasing the initial vapor density (and thus the pre-expansion temperature). Aside from the comparatively slight changes in diffusion coefficients, this will cause essentially two changes: (1) linearization of the vapor-temperature equilibrium boundary condition at a new point on the actual curve, and (2) a change in the value of C'. Assuming, as suggested by Table I, that final quasi steady-state droplet temperature is attained "instantaneously", the validity of the quasi steady-state solutions then depends primarily upon the radial increment, since this determines the time "allowed" for the transients to die out. A supersaturation which is augmented by increasing the initial density (keeping the initial temperature the same) has the general effect of decreasing b, since the final temperature and density are increased, and lie on a flatter part of the vapor-temperature equilibrium curve. The decrease in b gives rise to a slower approach to equilibrium; however for very small

droplets this retardation is virtually undetectable, and the initial mass influx in such cases appears to be rather insensitive to changes in b. For longer times higher final density must lead to a smaller mass influx (for a given initial density). Thus, since we are interested in an upper limit to the mass influx relinearization will be discounted as a deciding factor in its evaluation. This attributes the increase in mass influx to the increase in initial vapor density, ρ_0, which gives rise to an increase in:

$$|c'| = |bT_0 - \rho_0 + c|.$$

But c' can be factored out of the equation for mass influx so that one can write,

$$\frac{\left(\frac{dm}{dt}\right)_1}{\left(\frac{dm}{dt}\right)_2} = \frac{c_1'}{c_2'}. \tag{4.8}$$

Returning now to Table I, and recalling the argument presented at the top of page 49, it may be verified from (4.8) that the mass influx can still be restricted to 24% in a time of 10^{-5} seconds even if supersaturations of 10 are achieved.

Conclusions:

The fixed radius (macroscopic) solutions appear to justify steady-state methods down to drop sizes of the order of a mean free path. In this region, however, the macroscopic treatment breaks down, and kinetic theory

methods must be employed. For larger heterogeneous nuclei, the transient phase can be treated by the fixed radius solution and the subsequent steady-state phase by steady-state theory.

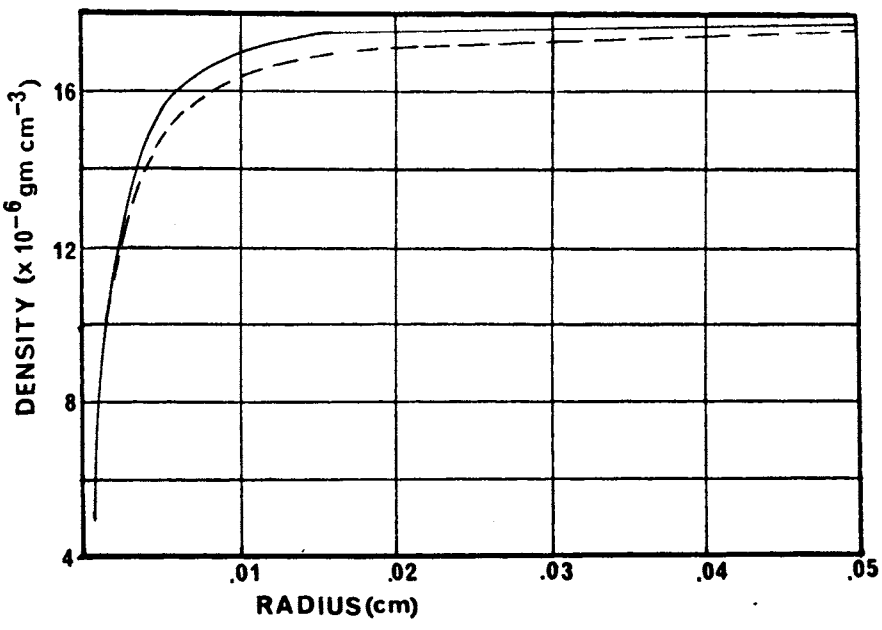

Figure 3. Vapor Density vs. Radius for a = 10 microns, $t = 10^{-4}$ seconds. ———Transient, -----Quasi Steady-State.

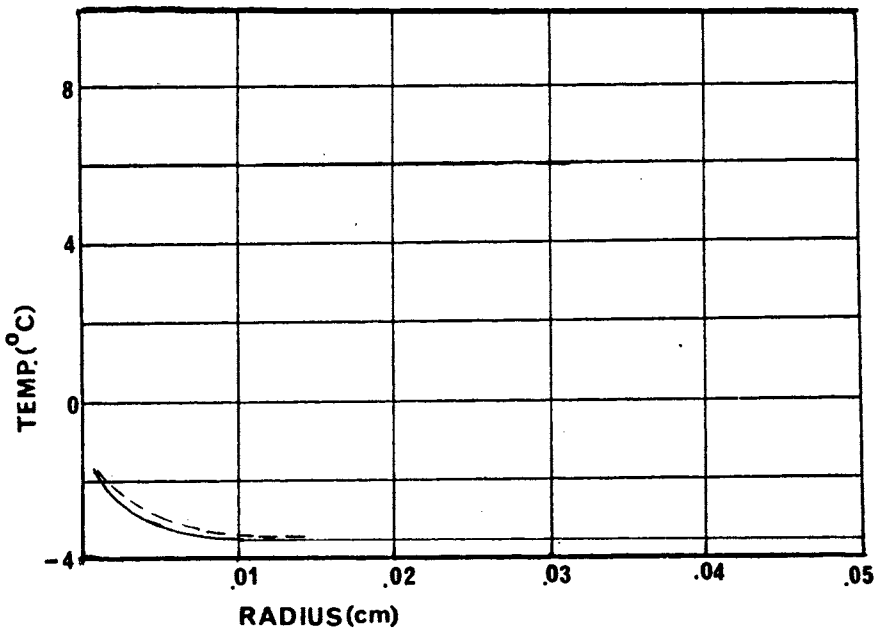

Figure 4. Temperature vs. Radius for a = 10 microns $t = 10^{-4}$ seconds. ——— Transient, ----- Quasi Steady-State.

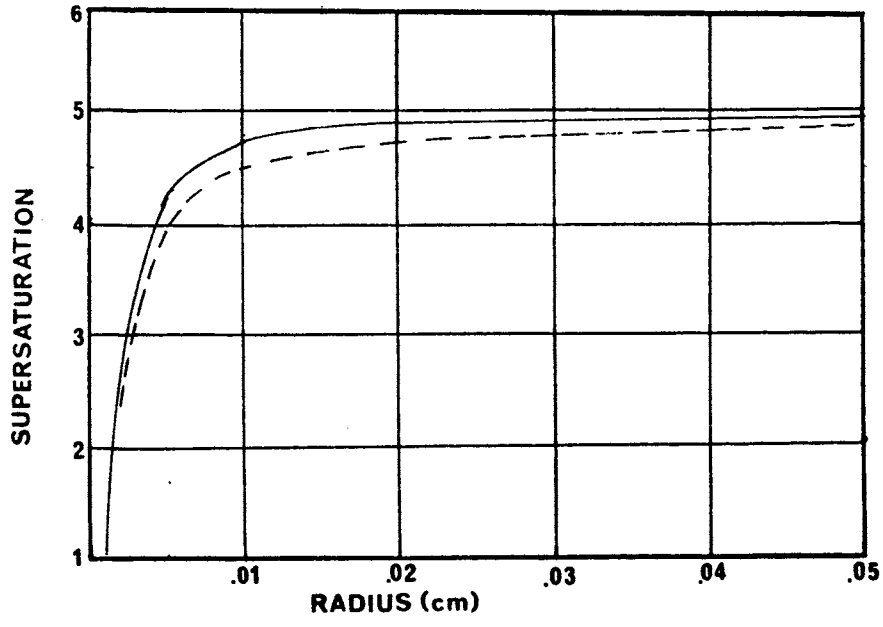

Figure 5. Supersaturation vs. Radius for a = 10 microns, $t = 10^{-4}$ seconds. ———Transient, -----Quasi Steady-State.

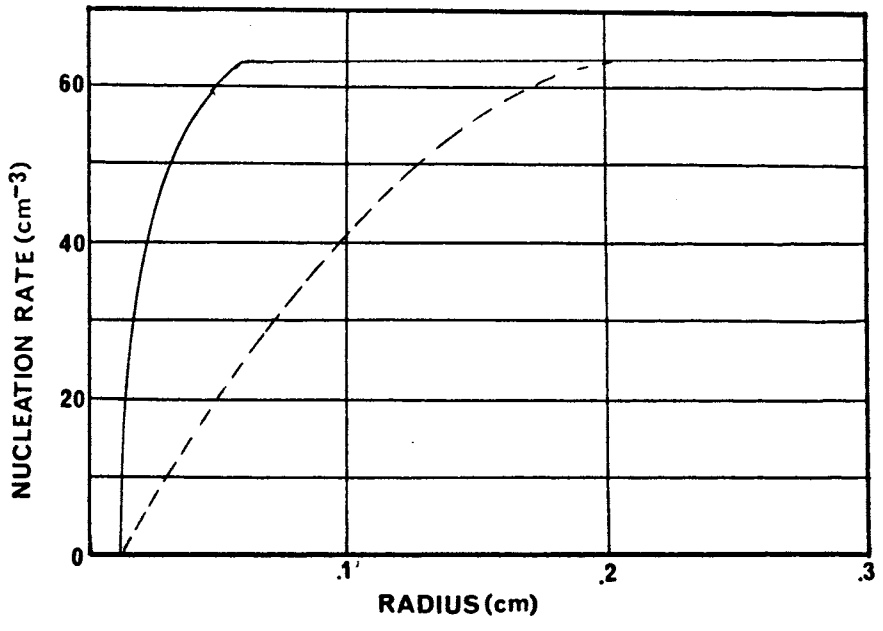

Figure 6. Nucleation Rate vs. Radius for a = 10 microns, $t = 10^{-4}$ seconds. ———Transient, ----- Quasi Steady-State. Dotted lines show dead space.

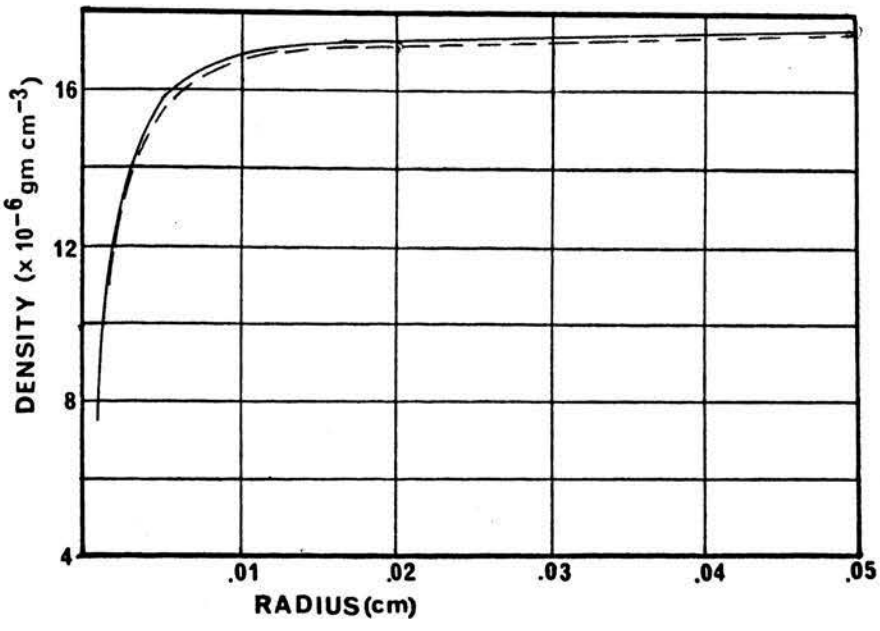

Figure 7. Vapor Density vs. Radius for a = 10 microns, $t = 10^{-3}$ seconds. ———Transient, -----Quasi Steady-State.

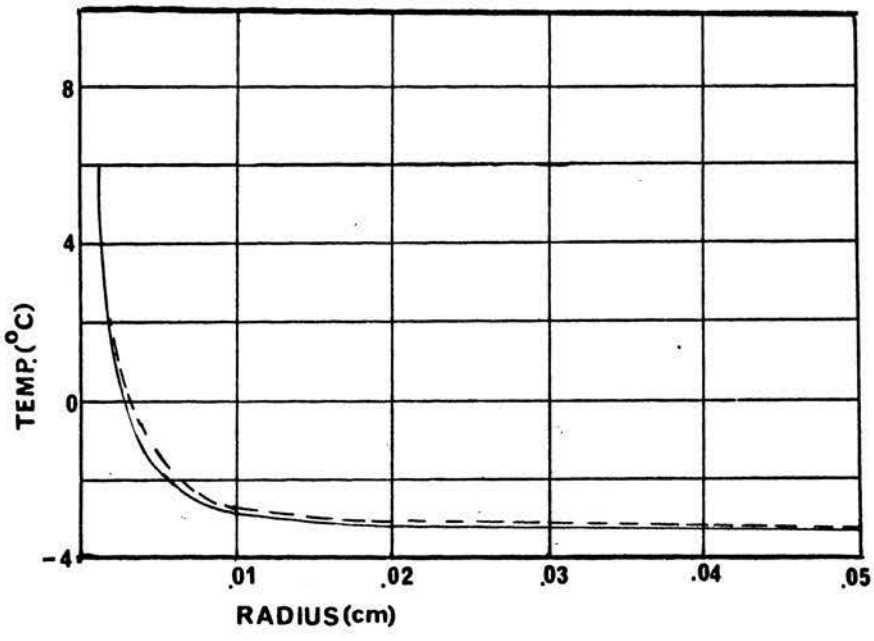

Figure 8. Temperature vs. Radius for a = 10 microns, $t = 10^{-3}$ seconds. ———Transient, -----Quasi Steady-State.

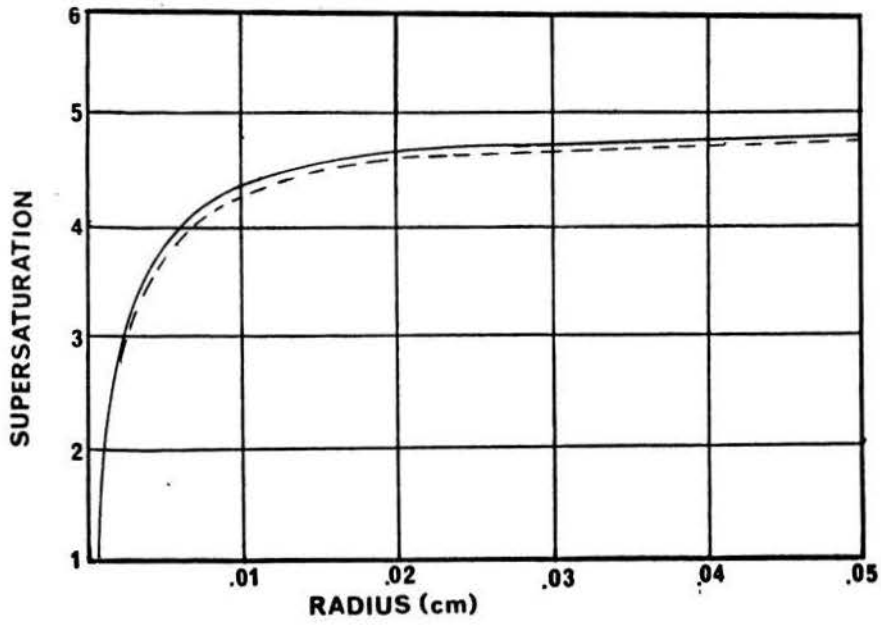

Figure 9. Supersaturation vs. Radius for a = 10 microns, $t = 10^{-3}$ seconds. ———Transient, -----Quasi Steady-State.

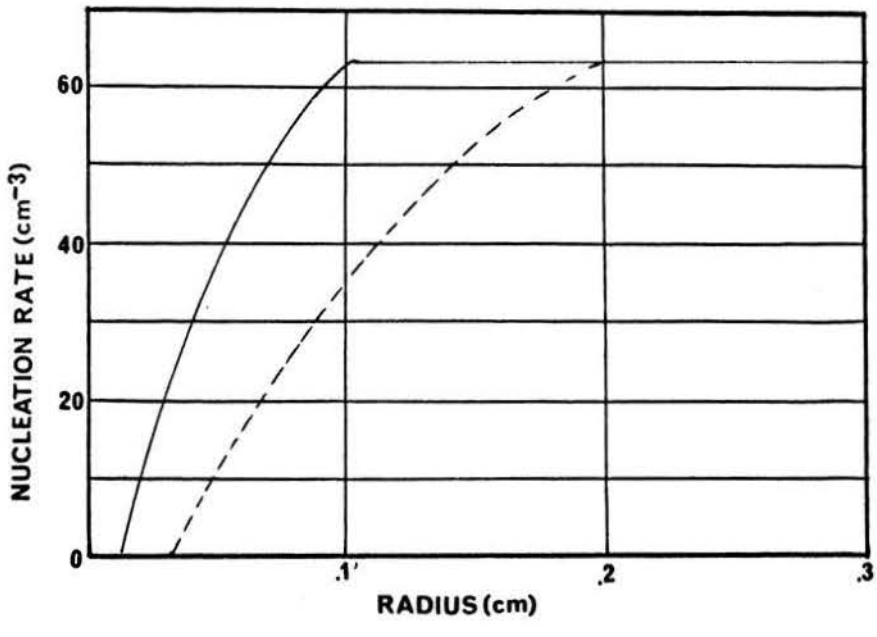

Figure 10. Nucleation Rate vs. Radius for a = 10 microns, $t = 10^{-3}$ seconds. ———Transient, -----Quasi Steady-State. Dotted lines show dead space.

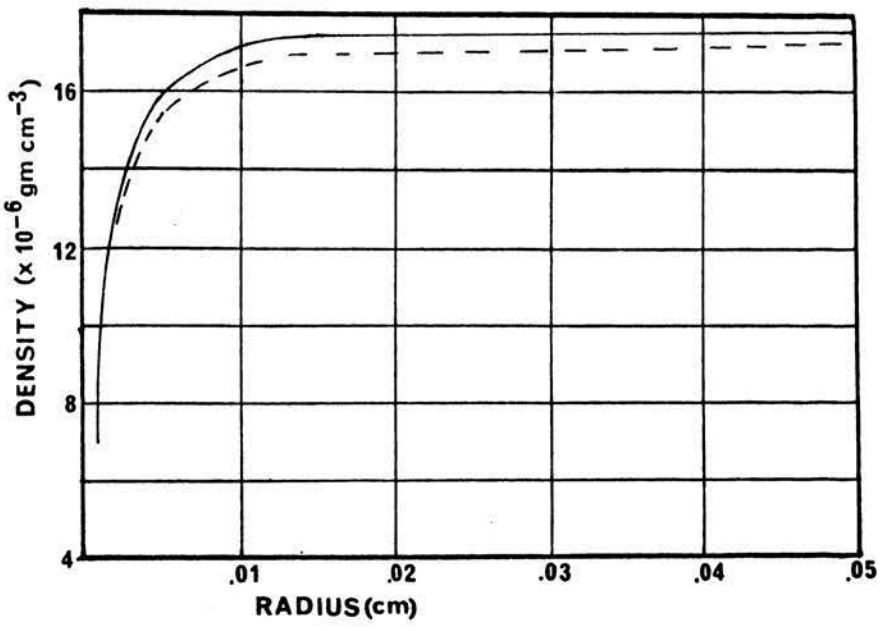

Figure 11. Vapor Density vs. Radius for a = 10 microns, $t = 10^{-4}$ seconds. $T(a,0) = -.1°C$, $T(r,0) = -3.6°C$. ———Transient, -----Quasi Steady-State.

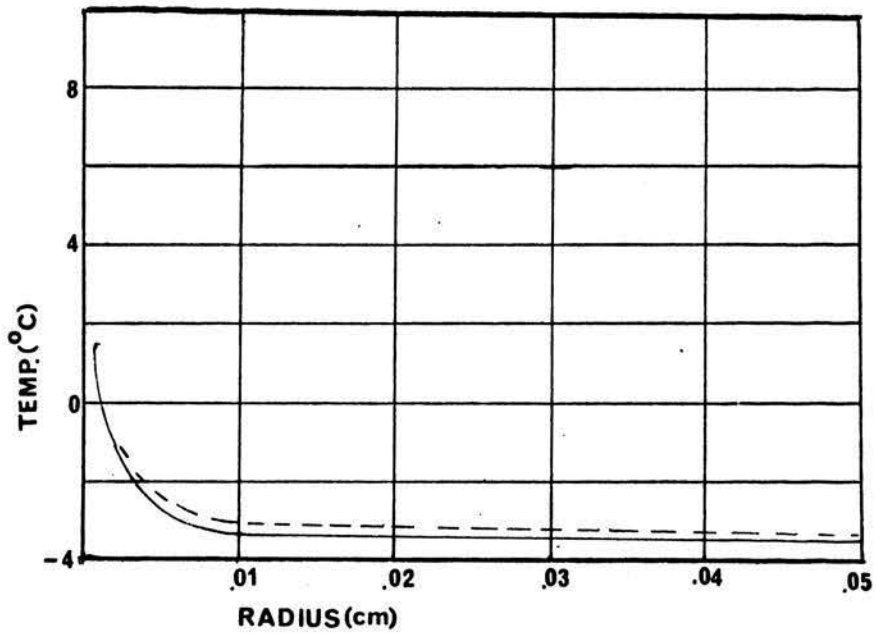

Figure 12. Temperature vs. Radius for a = 10 microns, $t = 10^{-4}$ seconds. $T(a,0) = -1°C$, $T(r,0) = -3.6°C$. ———Transient, -----Quasi Steady-State.

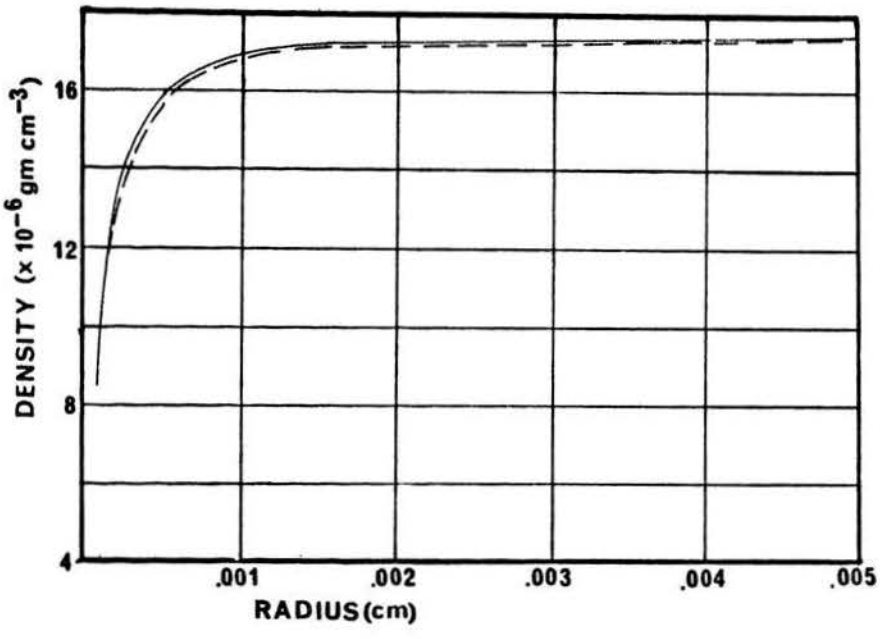

Figure 13. Vapor Density vs. Radius for a = 1 micron, $t = 10^{-5}$ seconds. $T(a,0) = -.1°C$, $T(r,0) = -3.6°C$. ———Transient, -----Quasi Steady-State.

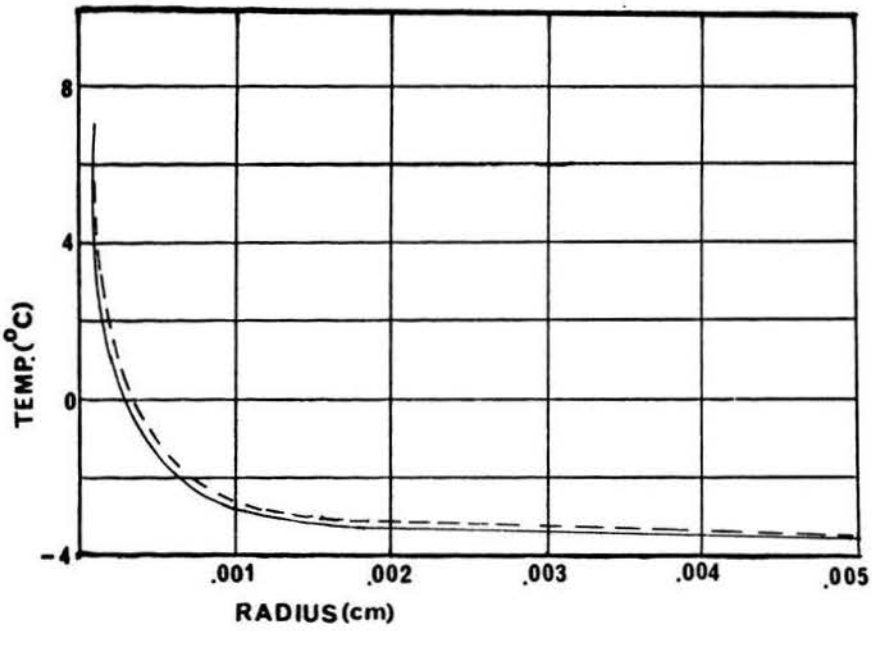

Figure 14. Temperature vs. Radius for a = 1 micron, $t = 10^{-5}$ seconds. $T(a,0) = -.1°C$, $T(r,0) = -3.6°C$. ———Transient, -----Quasi Steady-State.

TABLE I

Density Profiles for Fixed Radius Solution and for Steady-State Solutions

1	2	3	4	5	6	7
r (cm.)	$t=10^{-5}$(sec.)	$t=2\times10^{-5}$	$t=5\times10^{-5}$	$t=10^{-4}$	$\rho_{ss}(a)$	$\rho_{ss}(a+\Delta)$
.00005	8.65	8.66	8.65	8.65	8.66	8.66
.00008	12.10	12.08	12.08	12.08	12.08	12.03
.00010	13.25	13.23	13.23	13.22	13.22	13.18
.00015	14.78	14.75	14.75	14.47	14.73	14.71
.00025	16.00	15.97	15.97	15.96	15.95	15.93
.00040	16.69	16.65	16.65	16.64	16.63	16.62
.00070	17.18	17.15	17.15	17.13	17.12	17.11
.02000	17.76	17.76	17.76	17.75	17.75	17.75

Density profiles for fixed radius solution (columns 2-5) and for steady-state solutions (columns 6 and 7). Density is given in units of 10^{-6} gms/cm^3 and r in cm. Droplet radius is .5 microns (a = .00005 cm) for all calculations except those of column 7 where a has been increased by 8% corresponding to the amount of mass increase at the end of 2×10^{-5} seconds.

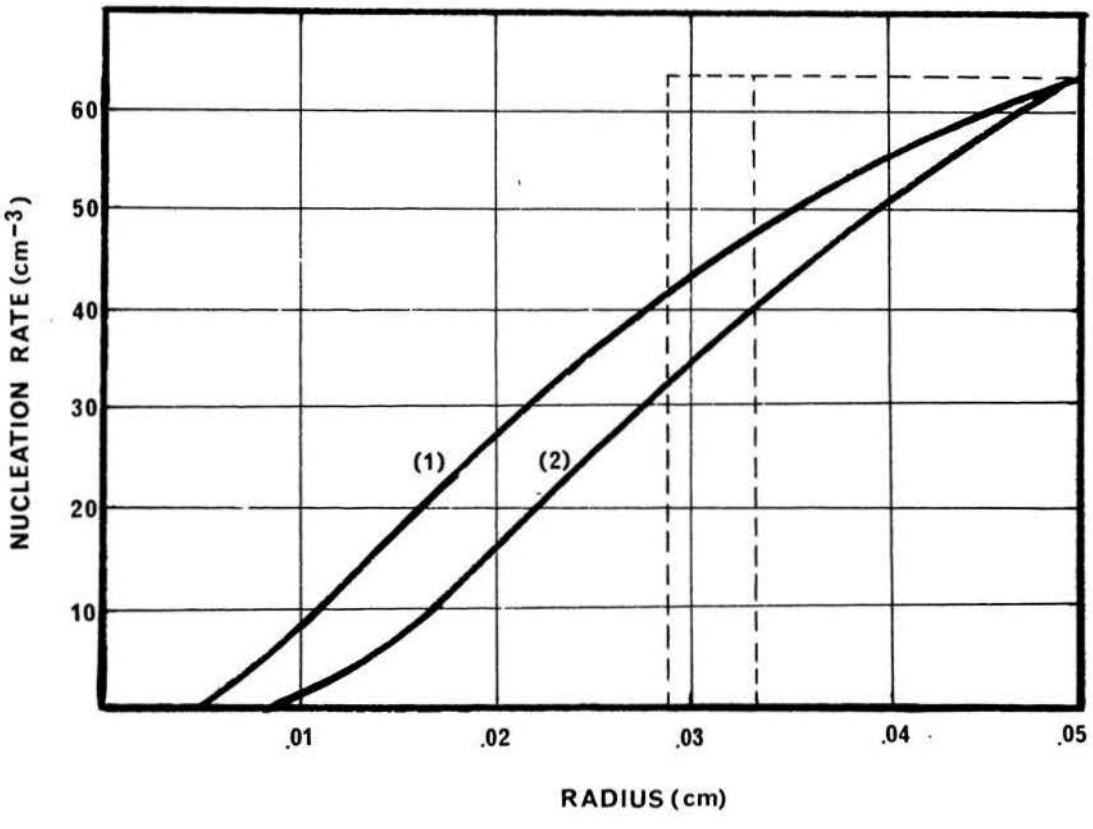

Figure 15. Becker-Doring Nucleation Rate as a Function of Radius, calculated from Quasi Steady-State Theory.

Curve (1)	t = .005 sec.	Curve (2)	t = .015 sec.
	a(t) = 2.19 mic.		a(t) = 3.73 mic.
	d(t) = .029 cm.		d(t) = .033 cm.

In each case the initial drop radius is .5 micron, and the radius of the outer sphere .05 cm. Dotted lines show dead space.

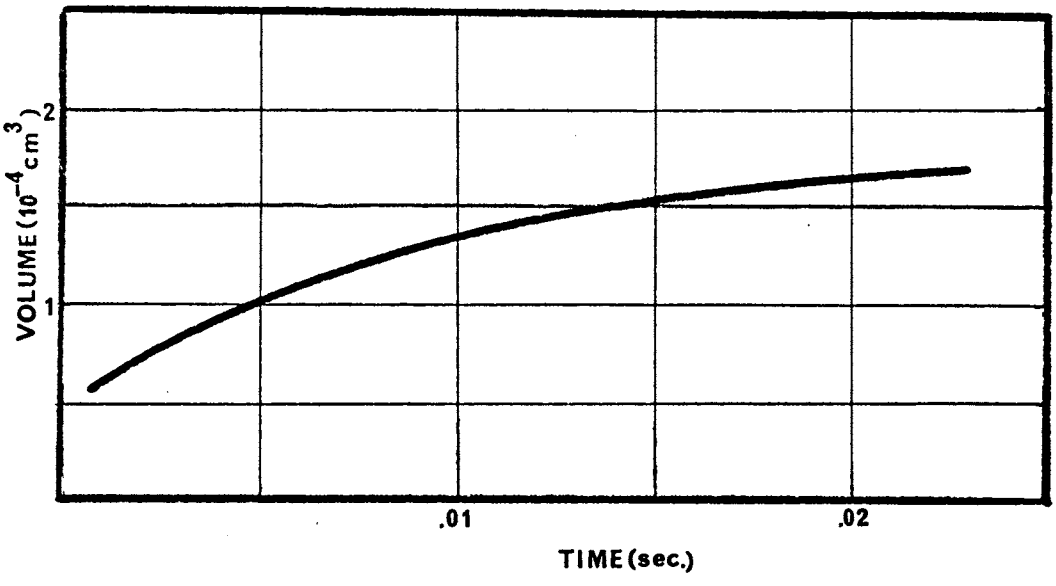

Figure 16. Dead Volume vs. Time calculated from Quasi Steady-State Theory for Becker-Doring Nucleation Rates.

APPENDIX I

The transforms of $\Xi_k(p,r)$ and $\chi_D \Xi_k(p,r)$, etc. (defined in Chapter III, pages 30 and 31) have been worked out by direct use of the inversion integral whose contour is shown in Figure 2 (page 29). The inverse is given as a sum of residues enclosed by the contour ABCDE. Such an inverse is valid if it can be shown that the integrand vanishes along the contour ABCDE. To do this consider the inversion:

$$L^{-1} \chi_D \Xi_k(p,r).$$

The contour will be split into two parts. The first part is the semi-circle BCD including the point x = 0, where the complex variable is given by: $p = \rho e^{i\theta}$. Consider the expression:

$$\lim_{\rho \to \infty} \int \frac{|\chi_D|}{|q|} \left| \frac{\sinh \eta_k(r)}{\sinh \eta_k(a)} \right| \rho e^{i\theta} e^{\rho(\cos\theta + i\sin\theta)t} d\theta$$

where,

$$\frac{\sinh \eta_k(r)}{\sinh \eta_k(a)} = \frac{\sinh\sqrt{\frac{p}{k}}(R-r) - R\sqrt{\frac{p}{k}}\cosh\sqrt{\frac{p}{k}}(R-r)}{\sinh\sqrt{\frac{p}{k}}(R-a) - R\sqrt{\frac{p}{k}}\cosh\sqrt{\frac{p}{k}}(R-a)}$$

and,

$$\begin{Bmatrix} \sinh\sqrt{\frac{p}{k}}(R-r) \\ \cosh\sqrt{\frac{p}{k}}(R-r) \end{Bmatrix} = \frac{1}{2}\left[e^{\frac{R-r}{\sqrt{k}}\sqrt{\rho}\left(\cos\frac{\theta}{2} + i\sin\frac{\theta}{2}\right)} \mp e^{-\frac{R-r}{\sqrt{k}}\sqrt{\rho}\left(\cos\frac{\theta}{2} + i\sin\frac{\theta}{2}\right)} \right]$$

We have:

$$\lim_{\rho\to\infty} \left|\sin\sqrt{\frac{\rho}{k}}(R-r)\right| = \lim_{\rho\to\infty} \left|\cosh\sqrt{\frac{\rho}{k}}(R-r)\right| \leq \frac{1}{2} e^{\frac{R-r}{\sqrt{k}}\sqrt{\rho}\left|\cos\frac{\theta}{2}\right|}$$

hence,

$$\lim_{\rho\to\infty} \left|\frac{\sinh\eta_k(r)}{\sinh\eta_k(a)}\right| \leq e^{\sqrt{\frac{\rho}{k}}(a-r)} \leq 1.$$

Now consider:

$$\chi_D(a) = \sqrt{\frac{\rho}{D}}\left[\frac{1-\sqrt{\frac{\rho}{D}}R\tanh\sqrt{\frac{\rho}{D}}(R-a)}{\tanh\sqrt{\frac{\rho}{D}}(R-a)-R\sqrt{\frac{\rho}{D}}}\right].$$

Excluding temporarily the negative real axis ($\theta\neq\pi$), the limit can be written:

$$\lim_{\rho\to\infty} \tanh\sqrt{\frac{\rho}{D}}(R-a) = \begin{cases} 1, & \frac{\pi}{4} \leq \frac{\theta}{2} < \frac{\pi}{2} \\ -1, & \frac{\pi}{2} < \frac{\theta}{2} \leq \frac{3\pi}{4}. \end{cases}$$

Therefore with these restrictions,

$$\lim_{\rho\to\infty} \left|\chi_D(a)\right| = \left|\frac{1}{a} \pm \sqrt{\frac{\rho}{D}}\right| \leq \left|\sqrt{\frac{\rho}{D}}\right| + \frac{1}{a}$$

Finally consider:

$$g(\rho) = \rho + \frac{\beta+b\alpha}{a} + \sqrt{\frac{\rho}{k}}\coth\eta_k(a) + \sqrt{\frac{\rho}{D}}\coth\eta_D(a)$$

as before with $\theta\neq\pi$.

$$\lim_{\rho\to\infty} g = \rho(\cos\theta+i\sin\theta) + \frac{\beta+b\alpha}{a} \pm \left(\frac{1}{\sqrt{k}}+\frac{1}{\sqrt{D}}\right)\sqrt{\rho}\left(\cos\frac{\theta}{2}+i\sin\frac{\theta}{2}\right)$$

$$\lim_{\rho\to\infty}|g| > \sqrt{\left[\rho\cos\theta-\sqrt{\rho}\left(\frac{1}{\sqrt{k}}+\frac{1}{\sqrt{D}}\right)\cos\frac{\theta}{2}\right]^2+\left[\rho\sin\theta-\sqrt{\rho}\left(\frac{1}{\sqrt{k}}+\frac{1}{\sqrt{D}}\right)\sin\frac{\theta}{2}\right]^2}$$

Hence along the contour the original integrand will be less than:

$$\frac{\left(\left|\sqrt{\frac{\rho}{D}}\right|+\frac{1}{a}\right)\rho\, e^{t\rho\cos\theta}}{\left\{\left[\rho\cos\theta-\sqrt{\rho}\left(\frac{1}{\sqrt{k}}+\frac{1}{\sqrt{D}}\right)\cos\frac{\theta}{2}\right]^2+\left[\rho\sin\theta-\sqrt{\rho}\left(\frac{1}{\sqrt{k}}+\frac{1}{\sqrt{D}}\right)\sin\frac{\theta}{2}\right]^2\right\}^{\frac{1}{2}}}$$

Consider the contour integral:

$$\int\frac{\left(\left|\sqrt{\frac{\rho}{D}}\right|+\frac{1}{a}\right)e^{t\rho\cos\theta}\,d\theta}{\left\{\left[\cos\theta-\frac{1}{\sqrt{\rho}}\left(\frac{1}{\sqrt{k}}+\frac{1}{\sqrt{D}}\right)\cos\frac{\theta}{2}\right]^2+\left[\sin\theta-\frac{1}{\sqrt{\rho}}\left(\frac{1}{\sqrt{k}}+\frac{1}{\sqrt{D}}\right)\sin\frac{\theta}{2}\right]^2\right\}^{1/2}}.$$

In the limit $\rho\to\infty$, this becomes:

$$\int\sqrt{\frac{\rho}{D}}\,e^{t\rho\cos\theta}\,d\theta$$

which is even in θ around the point π.

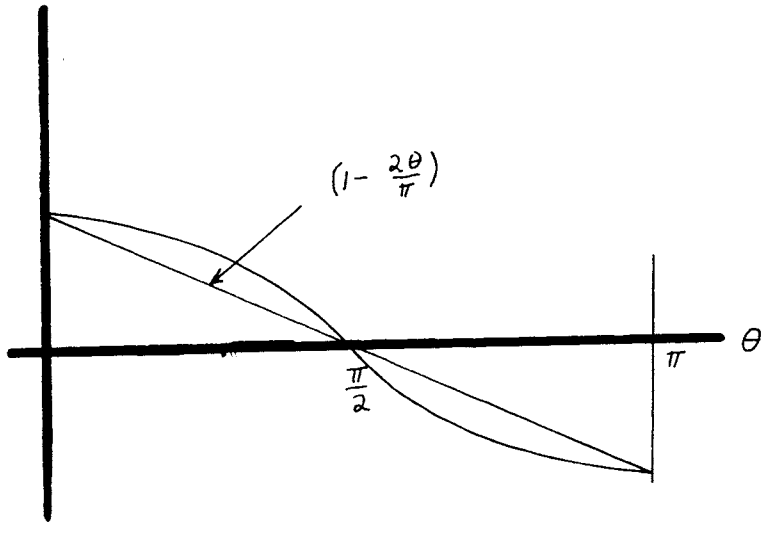

Figure 17. Geometrical demonstration of the inequality: $\cos\theta \leqq 1-\frac{2\theta}{\pi}$, $\frac{\pi}{2}\leq\theta\leq\pi$.

Within the limits of integration,

$$e^{\rho\cos\theta} \leqq e^{(1-\frac{2\theta}{\pi})\rho}.$$ (See Figure 17)

and direct integration between $\frac{\pi}{2}$ and π gives:

$$\frac{1-e^{-\rho}}{\sqrt{D\rho}} \xrightarrow[\rho \to \infty]{} 0.$$

The magnitude of ρ can be chosen so that the value of the integrand for large ρ along the negative real axis (which was excluded above) is as small as desired. In this special case $p = -\rho$. The integrand is:

$$\frac{\chi_D(-\rho,a)}{-\rho+\beta\chi_D(-\rho,a)+b\alpha\chi_K(-\rho,a)} \left.\frac{\sinh\eta_k(r)}{\sinh\eta_k(a)}\right|_{p=-\rho} e^{-\rho t}$$

which goes to zero at large ρ except when ρ is a root of $g(\rho)$.

Now if $p = x \pm i\rho$, then $\sqrt{p} = A + iB$, where

$$A = \frac{1}{\sqrt{2}}\sqrt{x \pm \sqrt{x^2+\rho^2}},$$

$$B = \frac{1}{\sqrt{2}}\sqrt{-x \pm \sqrt{x^2+\rho^2}}.$$

As was done previously:

$$\lim_{\rho\to\infty}\frac{\sinh\eta_k(r)}{\sinh\eta_k(a)} = \frac{e^{(R-r)/\sqrt{K}\,(A+iB)}}{e^{(R-a)/\sqrt{K}\,(A+iB)}}$$

whose maximum value is 1.

Next:

$$\chi_D = \sqrt{\frac{p}{D}}\,\frac{1-\sqrt{\frac{p}{D}}R\tanh\sqrt{\frac{p}{D}}(R-a)}{\tanh\sqrt{\frac{p}{D}}(R-a)-R\sqrt{\frac{p}{D}}} + \frac{1}{a}$$

$$\tanh\frac{R-a}{\sqrt{D}}\sqrt{p} \xrightarrow[\rho\to\infty]{} \pm 1$$

Finally,

$$g = \alpha + i\rho + \frac{\beta + b\alpha}{a} + \sqrt{\frac{P}{k}} \coth \eta_k(a) + \sqrt{\frac{P}{D}} \coth \eta_D(a)$$

from previous work, the coth terms can take on values ± 1, as $\rho \longrightarrow \infty$, and letting,

$$C_o' = \alpha + \frac{\beta + b\alpha}{a}$$

one obtains:

$$g(P) = i\rho \pm \left(\frac{1}{\sqrt{k}} + \frac{1}{\sqrt{D}}\right)(A + iB) + C_o'$$

$$\therefore \quad |g(P)| = \left\{ \left[C_o' \pm \left(\frac{1}{\sqrt{k}} + \frac{1}{\sqrt{D}}\right)A\right]^2 + \left[\rho \pm \left(\frac{1}{\sqrt{k}} + \frac{1}{\sqrt{D}}\right)B\right]^2 \right\}^{\frac{1}{2}}.$$

As $\rho \longrightarrow \infty$ the entire integrand is seen to become proportional to $\frac{1}{\sqrt{\rho}}$.

The other inverse, $L^{-1}\mathfrak{Z}_k(P,r)$ can be treated in the same fashion and its contribution to the contour ABCDE is also seen to vanish.

APPENDIX II

The nature of the roots of g(p), that is whether they are real, complex, or pure imaginary, is most straightforwardly determined by means of a plot in the complex plane. This plot can be localized somewhat, for a given problem, according to the inequalities which are developed in this Appendix.

From g(p) = 0, where z = p , we have:

$$-z - C_0/z = A_0 \coth(a_0 z - \tanh^{-1} a_0' z) + B_0 \coth(b_0 z - \tanh^{-1} b_0' z).$$

By means of the formulae:

$$\tanh^{-1} z = \frac{1}{2} \ln \frac{1+z}{1-z}$$

$$\ln z = \ln|z| \pm i(\theta + 2k\pi), \quad k = 0, 1, 2 \ldots$$

and,

$$\coth z = \frac{\sin 2x - i \sin 2y}{\cos 2x - \cos 2y} \qquad (z = x + iy)$$

this equation can be reduced to:

$$-\left(1 + \frac{C_0}{x^2+y^2}\right) + iy\left(\frac{C_0}{x^2+y^2} - 1\right) = A_0 \frac{\sinh 2(a_0 x - \frac{\gamma_a}{2}) - i \sin 2(a_0 y - \frac{\Delta\phi_a}{2})}{\cosh 2(a_0 x - \frac{\gamma_a}{2}) - \cos 2(a_0 y - \frac{\Delta\phi_a}{2})}$$

$$+ B_0 \frac{\sinh 2(b_0 x - \frac{\gamma_b}{2}) - i \sin 2(b_0 y - \frac{\Delta\phi_b}{2})}{\cosh 2(b_0 x - \frac{\gamma_b}{2}) - \cos 2(b_0 y - \frac{\Delta\phi_b}{2})}$$

where,

$$\zeta_a = \frac{1}{2} \ln\left[\frac{(1+a_o'x)^2+(a_o'y)^2}{(1-a_o'x)^2+(a_o'y)^2}\right]$$

and,

$$\Delta\phi_a = \tan^{-1}\frac{y}{x+1/a_o'} - \tan^{-1}\frac{y}{x-1/a_o'}$$

Equating real parts of this equation gives:

$$-x\left(1+\frac{c_o}{x^2+y^2}\right) = A_o \frac{\sinh 2(a_o x - \zeta_a/2)}{\cosh 2(a_o x - \zeta_a/2) - \cos 2(a_o y - \frac{\Delta\phi_a}{2})}$$

$$+ B_o \frac{\sinh 2(b_o x - \zeta_b/2)}{\cosh 2(b_o x - \frac{\zeta_b}{2}) - \cos 2(b_o y - \frac{\Delta\phi_b}{2})}.$$

The denominators of the right-hand terms are always positive, hence at least one of the right-hand numerators must agree with the left-hand term in sign. This requires $x \geqq 0$, and leads to the inequalities:

$$2a_o x \leqq \ln\left[\frac{(1+a_o'x)^2+(a_o'y)^2}{(1-a_o'x)^2+(a_o'y)^2}\right]$$

$$2b_o x \leqq \ln\left[\frac{(1+b_o'x)^2+(b_o'y)^2}{(1-b_o'x)^2+(b_o'y)^2}\right].$$

At least one of these inequalities must be satisfied for roots to exist.

If the possibility x = 0 is now excluded, and R is

taken to be .3 cm., a numerical evaluation of the above inequalities gives:

$$0 < x \leq 4.29$$

$$-3.57 < y < 3.57.$$

If, in addition, the inner radius is taken to be less than 20 microns, which for the present problem is always the case, we have $C_o/(x^2 + y^2) > 1$, so that the inequalities associated with the imaginary terms can be used, These are:

$$2a_o y < \tan^{-1}\frac{y}{x+1/a_o'} - \tan^{-1}\frac{y}{x-1/a_o'}$$

$$2b_o y < \tan^{-1}\frac{y}{x-1/b_o'} - \tan^{-1}\frac{y}{x-1/b_o'}.$$

For these inequalities the range of x is further reduced to:

$$3.57 < x < 4.29.$$

And this additional restriction on x leads, from the "real" inequalities, to a further restriction on y:

$$-1.2 < y < 1.2$$

The above ranges in x and y can now be substituted into g(z) and a plot of the region can be obtained with the help of the computer. Such plots imply that roots exist only for x = 0.

APPENDIX III

Some limits:

1. $$\lim_{P \to 0} \frac{\sinh \eta_k(r)}{\sinh \eta_k(a)} = \frac{r}{a}$$

where, $$\eta_k(r) = \sqrt{\frac{P}{k}}(R-r) - \tanh^{-1} R\sqrt{\frac{P}{k}}.$$

2. $$\lim_{P \to 0} \frac{P}{\chi_D(a)} = \frac{3Da^2}{R^3 - a^3}$$

where, $$\chi_D(a) = \sqrt{\frac{P}{D}} \coth \eta_D(a) + \frac{1}{a}.$$

3. $$\lim_{P \to 0} \frac{\chi_k(a)}{\chi_D(a)} = \frac{D}{k}.$$

APPENDIX IV

The "pulse" form of a cloud-chamber expansion can be approximated by a parabola:

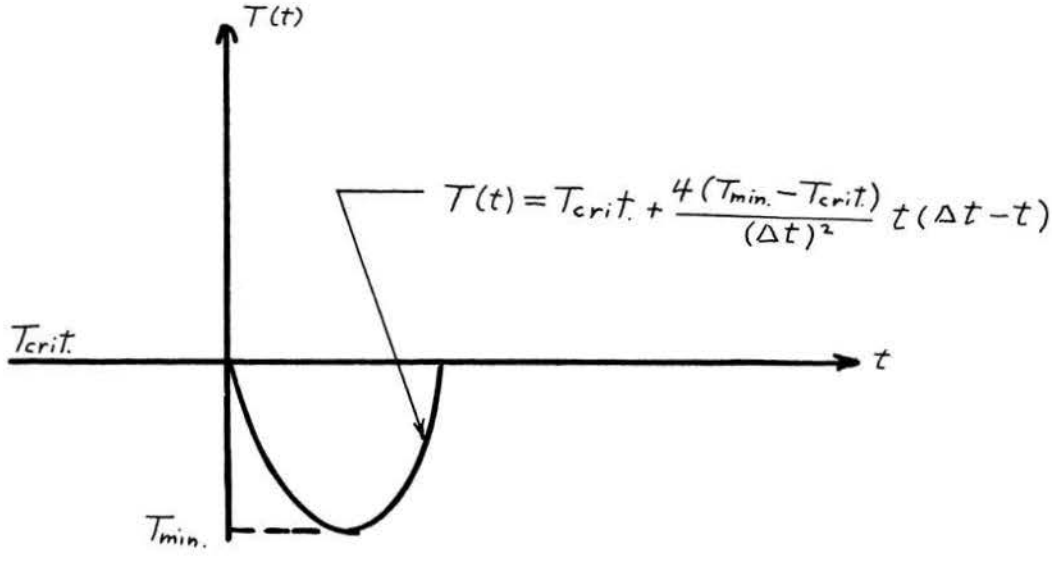

Figure 18. Postulated parabolic temperature dependence of cloud-chamber pulse.

The "sink" term is given by:

$$F_T(t) = \Gamma_T(\Delta t - 2t)$$

where,

$$\Gamma_T = \frac{4(T_{min.} - T_{crit.})}{(\Delta t)^2} .$$

A similar approximation holds for the density sink:

$$F_\rho(t) = \Gamma_\rho(\Delta t - 2t)$$

where,

$$\Gamma_\rho = \frac{4(\rho_{min.} - \rho_{crit.})}{(\Delta t)^2} .$$

APPENDIX V

A computer program is presented in this appendix which is designed to find the roots of g(iv). The smallest (first) root is calculated in a separate program with extra accuracy. Also presented is a list of equivalent fortran variables used in the programs presented in this Appendix and Appendix VII.

A LIST OF VARIABLES AND THEIR FORTRAN EQUIVALENTS

Variable Name	Fortran Equivalent
r	X(I)
t	T(J)
a	A
R	R
k	AK
D	AD
l	CNLAT
T_o	TEMPO
ρ_o	DENSO
T_a	TEMPA
ρ_a	DENSA
K	THERM
A_o	SA
B_o	SB
C_o	C
a_o	TA
b_o	TB
c	CINT
c'	CSCA
b	B
T	TEMP
ρ	RHO

```
*LIST PRINTER
*ALL STATEMENT MAP
C  C***01249PHX006  J CARSTENS          12/09/65 FORTRAN 2    0080 004 0
C      ROOTS OF G(V) USING INF. DISC AS 1ST. APPROXA(A=.5MIC.  R=.05CM)-
       DIMENSION YI(20), AN(20),Y(20),XS(2), XT(2)
       A=.00005
   999 FORMAT (I5)
   300 FORMAT (4E18.8)
    50 FORMAT(20F3.0)
       READ 200, THERM , CINTC,DENSO,TEMPO,CNLAT
       READ 200, R,AD,AK,B
       READ 50, (AN(J),J=1,10)
       ALPHA=3.*CNLAT*AD/A
       BETA=3.*THERM/A
       ALPHB=B*ALPHA
       CSCA=CINTC+B*TEMPO-DENSO
       C=(ALPHB+BETA)/A
       CSQ=SQRTF(C)
       PRINT 300, BETA,ALPHA,CSCA
   200 FORMAT (5E14.6)
       SQD=SQRTF(AD)
       SQK=SQRTF(AK)
       AO=BETA/SQK
       BO=ALPHB/SQD
       PRINT 200,B,BO,AO,C
       SA=(R-A)/SQK
       SB=(R-A)/SQD
       TA=R/SQK
       TB=R/SQD
       XS(1)=SA
       XS(2)=SB
       XT(1)=TA
       XT(2)=TB
       PRINT 300,SA,SB,TA,TB
       DO 31 JJ=1,2
       DO 9 J=1,10
       YI(J)=3.1416*(2.*AN(J)+1.)/(2.*XS(JJ))
       PRINT 200,YI(J),AN(J),XS(JJ)
       Y(J)=YI(J)
     1 Y(J)=Y(J)-.01
       N=1
       FYY=SINF(XS(JJ)*Y(J))/COSF(XS(JJ)*Y(J))-XT(JJ)*Y(J)
        IF (ABSF(FYY)-.0001) 9,9,2
     2 IF(FYY)3,9,1
     3 Y(J)=Y(J)+.01/(2.**N)
       IF(N-25)155,155,9
   155 N=N+1
       FYY=SINF(XS(JJ)*Y(J))/COSF(XS(JJ)*Y(J))-XT(JJ)*Y(J)
```

```
      IF (ABSF(FYY)-.0001) 9,9,4
    4 IF (FYY)3,9,5
    5 Y(J)=Y(J)-.01/(2.**N)
      IF(N-25)156,156,9
  156 N=N+1
      FYY=SINF(XS(JJ)*Y(J))/COSF(XS(JJ)*Y(J))-XT(JJ)*Y(J)
      IF (ABSF(FYY)-.0001) 9,9,6
    6 IF(FYY)3,9,5
    9 PRINT 200,Y(J),FYY
      DO 30 J=1,10
      L=1
      PRINT 999,J
      IF (CSQ-Y(J)) 10,10,1001
   10 HICUP=-1.0
      GO TO 1104
 1001 HICUP=1.0
 1104 X=Y(J)
   11 X=X-.05 *HICUP
      ARGB=SB*X-ATANF(TB*X)
      ARGA=SA*X-ATANF(TA*X)
      FX=C/X-X+AO*COSF(ARGA)/SINF(ARGA)+BO*COSF(ARGB)/SINF(ARGB)
 1105 IF (ABSF(FX)-.2) 29,29,1106
 1106 IF (CSQ-Y(J)) 1107,1107,12
 1107 IF (FX) 14,29,11
   12 IF(FX)11,29,17
   14 X=X-.05/(2.**L)
      L=L+1
      ARGA=SA*X-ATANF(TA*X)
      ARGB=SB*X-ATANF(TB*X)
      FX=C/X-X+AO*COSF(ARGA)/SINF(ARGA)+BO*COSF(ARGB)/SINF(ARGB)
      IF(ABSF(FX)-.2) 29,29,15
   15 IF(L-30) 16,16,29
   16 IF(FX)14,29,17
   17 X=X+.05/(2.**L)
      ARGA=SA*X-ATANF(TA*X)
      ARGB=SB*X-ATANF(TB*X)
      FX=C/X-X+AO*COSF(ARGA)/SINF(ARGA)+BO*COSF(ARGB)/SINF(ARGB)
      L=L+1
      IF(ABSF(FX)-.2) 29,29,18
   18 IF (L-30) 19,19,29
   19 IF(FX)14,29,17
   29 XSQ=X*X
   30 PRINT 300,X,FX,XSQ
   31 CONTINUE
C     NOW CALCULATE SPECIAL ROOT
      X=SQRTF(C)
```

```
      M=1
      ARGA=SA*X-ATANF(TA*X)
      ARGB=SB*X-ATANF(TB*X)
      FX=C/X-X+AO*COSF(ARGA)/SINF(ARGA)+BO*COSF(ARGB)/SINF(ARGB)
      IF(FX) 6003,79,6001
 6001 X=X+.5
      ARGA=SA*X-ATANF(TA*X)
      ARGB=SB*X-ATANF(TB*X)
      FX=C/X-X+AO*COSF(ARGA)/SINF(ARGA)+BO*COSF(ARGB)/SINF(ARGB)
      IF(ABSF(FX)-.001) 79,79,6002
 6002 IF(FX) 63,79,6001
 6003 X=X-.5
      ARGA=SA*X-ATANF(TA*X)
      ARGB=SB*X-ATANF(TB*X)
      FX=C/X-X+AO*COSF(ARGA)/SINF(ARGA)+BO*COSF(ARGB)/SINF(ARGB)
      IF (ABSF(FX)-.001) 79,79,6004
 6004 IF(FX) 6003,79,60
   60 X=X+.5/(2.**M)
      M=M+1
      ARGA=SA*X-ATANF(TA*X)
      ARGB=SB*X-ATANF(TB*X)
      FX=C/X-X+AO*COSF(ARGA)/SINF(ARGA)+BO*COSF(ARGB)/SINF(ARGB)
      IF (ABSF(FX)-.001) 79,79,61
   61 IF ( M-25)62,62,79
   62 IF(FX)63,79,60
   63 X=X-0.5/(2.**M)
      ARGA=SA*X-ATANF(TA*X)
      ARGB=SB*X-ATANF(TB*X)
      FX=C/X-X+AO*COSF(ARGA)/SINF(ARGA)+BO*COSF(ARGB)/SINF(ARGB)
      M=M+1
      IF(M-25) 64,64,79
   64 IF(ABSF(FX)-.001)79,79,65
   65 IF(FX)63,79,60
   79 XSQ=X*X
      PRINT 300,X,XSQ,FX,CSQ
      CALL EXIT
      END
```

```
C  C***95644PHX006  J CARSTENS          11/22/65 FORTRAN 2    0040 001 0
C      IST ROCT...EXTRA ACC.  (A=5  MICROM)
  200 FORMAT (5E14.6)
  300 FORMAT (4E18.8)
      A=.0005
      READ 200, THERM , CINTC,DENSO,TEMPO,CNLAT
      READ 200, R,AD,AK,B
      ALPHA=3.*CNLAT*AD/A
      BETA=3.*THERM/A
      ALPHB=5*ALPHA
      CSCA=CINTC+B*TEMPO-DENSO
      PRINT 300, BETA,ALPHA,CSCA
      SOD=SQRTF(AD)
      SOK=SQRTF(AK)
      AO=BETA/SOK
      BO=ALPHB/SOD
      SA=(R-A)/SOK
      SB=(R-A)/SOD
      TA=R/SOK
      TB=R/SOD
      C=(BETA+ALPHB)/A
      PRINT 200, AO,BO,C
      PRINT 200, SA,SB,TA,TB
      W=SQRTF(3.*(TA-SA)/(SA**3))
      VINIT=SQRTF(3.*(TB-SB)/(SB**3))
      PRINT 200,VINIT,W
      N=1
      L=1
      V=VINIT
  401 V=V+.0001
      L=L+1
      IF(L-1000)402,402,419
  402 ARGA=SA*V-ATANF(TA*V)
      ARGB=SB*V-ATANF(TB*V)
      FV=C/V -V +AO*COSF(ARGA)/SINF(ARGA)+BO*COSF(ARGB)/SINF(ARGB)
      IF (FV)403,419,401
  403 IF(ABSF(FV )-1.)419,419,404
  404 V=V-.0001/(2.**N)
      IF (N-25  ) 4045,4045,419
 4045 N=N+1
      ARGA=SA*V-ATANF(TA*V)
      ARGB=SB*V-ATANF(TB*V)
      FV=C/V -V +AO*COSF(ARGA)/SINF(ARGA)+BO*COSF(ARGB)/SINF(ARGB)
      IF(ABSF(FV )-1.)419,419,405
  405 IF (FV) 404,419,406
```

```
  406 V=V+.0001/(2.**I)
      IF (I-25  ) 4065,4065,419
 4065 I=I+1
      ARGA=SA*V-ATAN(TA*V)
      ARGB=SB*V-ATAN(TB*V)
      FV=C/V -V +A0*COSF(ARGA)/SINF(ARGA)+B0*COSF(ARGB)/SINF(ARGB)
      IF(ABSF(FV)-.1)419,419,407
  407 IF (FV) 404,419,406
  419 PRINT 200,V,FV
      VSQ=V*V
      PRINT 200,VSQ
      X=V
      TANSA=SINF(SA*X)/COSF(SA*X)
      TANSB=SINF(SB*X)/COSF(SB*X)
      DENA=TANSA-TA*X
      DENB=TANSB-TB*X
      FX=C/X-X+A0*(1.+TA*X*TANSA)/DENA + B0*(1.+TB*X*TANSB)/DENB
      PRINT 200, X,FX
      CALL EXIT
      END
```

APPENDIX VI

The following program is designed to evaluate the temperature as given in equation (4.6) on page 44 (see also expressions 4.1 and 4.2 on page 41). The "computer" variables are the same as those used in Appendix V. Similar programs were used to evaluate both the density and mass influx.

```
*LIST PRINTER
*ALL STATEMENT MAP
*FANDK1204
C  C***00943PHX006  J CARSTENS          12/08/65 FORTRAN 2    0030 006 0
C       TEMP. CALC. (A=1  MICRON, R=.05 CM.)
        DIMENSION C(30),P(30),CD(30,30),X(30), T(30), EXT(30,30),CSINK(30)
        A=.0001
        READ 1,N,M,L
        READ 400,(X(I),I=1,N)
        READ 400,(T(J),J=1,M)
        READ 200, THERM, CINTC,DENSO,TEMPO,CNLAT
        READ 200, R,AD,AK,B
        READ 100, (P(K),K=1,L)
    200 FORMAT (5E14.6)
    300 FORMAT (4E18.8)
        ALPHA=3.*CNLAT*AD/A
        BETA=3.*THERM/A
        ALPHB=B*ALPHA
        CSCA=CINTC+B*TEMPO-DENSO
        PRINT 300, BETA, ALPHA,CSCA
        ALPHC=ALPHA*CSCA
        PRINT 300,ALPHC
        SQD=SQRTF(AD)
        SQK=SQRTF(AK)
        AO=BETA/SQK
        BO=ALPHB/SQD
        SA=(R-A)/SQK
        SB=(R-A)/SQD
        TA=R/SQK
        TB=R/SQD
        PRINT 300,SA,SB,TA,TB
        DO 41 K=1,L
        ETAK=(R-A)*SQRTF(P(K)/AK)-ATANF(R*SQRTF(P(K)/AK))
        ETAD=(R-A)*SQRTF(P(K)/AD)-ATANF(R*SQRTF(P(K)/AD))
        COTK=COSF(ETAK)/SINF(ETAK)
        COTD=COSF(ETAD)/SINF(ETAD)
        DX1KO=-1.*COTK/(2.0*SQRTF(P(K)*AK))
        DX1KT=(R-A-R/(1.+R*R*P(K)/AK))*1./(2.*AK*(SINF(ETAK))**2)
        DX1DO=-1.*COTD/(2.0*SQRTF(P(K)*AD))
        DX1DT=(R-A-R/(1.+R*R*P(K)/AD))*1./(2.0*AD*(SINF(ETAD))**2)
        DX1K=DX1KO+DX1KT
        DX1D=DX1DO+DX1DT
        DG=1.+BETA*DX1K+ALPHB*DX1D
        C(K)=ALPHC*(COTD*SQRTF(P(K)/AD)+1./A )/(P(K)*DG)
        CSINK(K)=C(K)/SINF(ETAK)
     41 PRINT 300,P(K),C(K)
        DO 20 K=1,L
        CSQ=SQRTF(P(K)/AK)
```

```
      CAT=ATANF(R*CSQ)
      DO 10 I=1,N
      CD(I,K)=CSINK(K)*A*SINF((R-X(I))*CSQ-CAT)/X(I)
      IF(K-5) 411,411,10
  411 PRINT 300,CD(I,K)
   10 CONTINUE
   20 CONTINUE
      DO 40 K=1,L
      DO 30 J=1,M
      EXT(K,J)=1./EXPF(P(K)*T(J))
   30 CONTINUE
   40 CONTINUE
      DO 70 I=1,N
      DO 60 J=1,M
      TEMP=0.0
      DO 50 K=1,L
      CSQ=SQRTF(P(K)/AK)
      CAT=ATANF(R*CSQ)
      XA=X(I)
      TEMPP=CD(I,K)*EXT(K,J)
      IF(K-1)50,42,50
   42 PRINT 200,TEMPP
   50 TEMP=TEMP+TEMPP
   60 PRINT 200,T(J),X(I),TEMP
   70 CONTINUE
      PRINT 300, A0,B0
      CALL EXIT
    1 FORMAT (3I2)
  100 FORMAT (6F12.0)
  400 FORMAT (10F7.0)
      END
```

REFERENCES

1. E. F. Allard, "A New Determination of the Homogeneous Nucleation Rate of Water in Helium," Ph. D. Dissertation, University of Missouri at Rolla, 1965.

2. M. Grayson, Masters Thesis, University of Missouri at Rolla, 1965.

3. W. Courtney, Kinetics of Condensation from the Vapor Phase, Summary Report TM-1250, Texas Experiment, Inc., 1961.

4. E. F. Allard, op. cit., p. 45.

5. B. J. Mason, Proc. Phys. Soc., B 64, p. 773, (1951).

6. M. Neibuger and C. W. Chien, Computations of the Growth of Cloud Drops Using an Electronic Digital Computer, Geophysical Monograph No. 5, NAS-NRC Am. Geophys. Union, (1960).

7. H. Riess and V. K. La Mer, J. of Chem. Phys., 20, p. 1, (1950).

8. J. S. Kirkaldy, Can. Journ. of Physics., 36, p. 446, (1958).

9. M. Tsui, Geophys. Mag. 22, p. 11, (1950).

10. M. Neiburger and C. W. Chien, loc. cit.

11. V. E. Bagge, F. Becker, and G. Beckow, Z. Ang. Phy. 3, p. 13, (1951).

12. C. H. Kieth and A. B. Arons, J. of Meteor., 11, p. 173, (1954).

13. B. J. Mason, loc. cit.

14. R. Buecher, Masters Thesis, University of Missouri at Rolla, 1964, p. 18.

15. E. O. Barret and L. S. Germain, Rev. Sci. Instr., 18, p. 84, (1947).

16. W. E. Hazen, Rev. Sci. Instr., 18, p. 84, (1947).

17. B. J. Mason, loc. cit.

18. F. Frey, Z. Phys. Chem, 49B, p. 83, (1941).

19. V. E. Bagge, F. Becker, and G. Beckow, loc. cit.

20. H. L. Frisch and F. C. Collins, J. of Chem. Phys., 20, p. 1797, (1952).

21. L. Monchick and H. Riess, J. of Chem. Phys., 22, p. 831, (1954).

22. R. Buecher, loc. cit.

23. Ibid.

24. L. Monchick and H. Riess, loc. cit.

25. P. L. Chambre, Quart. J. of Mech. and Appl. Math., 9 (pt. II) p. 224, (1956).

26. J. Crank, The Mathematics of Diffusion, (Oxford at the Clarendon Press, 1957).

27. J. S. Kirkaldy loc. cit.

28. F. C. Frank, Proc. Roy. Soc., 201A, p. 586, (1950).

29. J. S. Kirkaldy, loc. cit.

30. H. Riess and V. K. La Mer, loc. cit.

31. R. Buecher, loc. cit.

32. F. J. M. Farley, proc. Roy. Soc., A212, p. 530, (1952).

33. R. Buecher, loc. cit.

34. E. J. Scott, Transform Calculus with an Introduction to Complex Variables, (Harper and Brothers, New York, 1955) p. 56.

35. Ibid. p. 23.

36. Ibid. p. 57.

37. Ibid. p. 32.

38. Ibid. p. 57.

39. Ibid. p. 57.

40. H. Riess and V. K. La Mer, loc. cit.

41. M. Grayson, Private communication.

42. F. A. Schwertz and J. E. Brow, J. of Chem. Phys., 19, p. 644, (1951).

43. V. E. Bagge, F. Becker, and G. Bekow, loc. cit.

44. International Critical Tables of Numerical Data, Physics, Chemistry, and Technology, (McGraw Hill Book Company, Inc., New York, 1926) 5.

45. R. Buecher op. cit., p. 19.

46. R. Becker and W. Doring, Ann. der Phys., 24, p. 719, (1935).

47. R. Buecher, loc. cit.

VITA

The author was born on October 8, 1937 in Chicago, Illinois. He received his primary education at Sutherland Public School, and his secondary education from Morgan Park High School in Chicago. The first year of his college education was received from Wilson Junior College in Chicago, and the remaining three years from Monmouth College in Monmouth, Illinois, where he received a BA degree in June 1959. He entered the University of Missouri at Rolla in September 1959.